STUDY OF THE EFFECT OF RARE EARTH IONS ON THE STRUCTURAL, MAGNETIC AND ELECTRICAL PROPERTIES OF Cu-Zn FERRITES

M. Sc. Thesis

BY

PRODIP KUMAR MONDAL

DEPARTMENT OF PHYSICS
KHULNA UNIVERSITY OF ENGINEERING & TECHNOLOGY
KHULNA - 9203, BANGLADESH
MAY - 2018

STUDY OF THE EFFECT OF RARE EARTH IONS ON THE STRUCTURAL, MAGNETIC AND ELECTRICAL PROPERTIES OF Cu-Zn FERRITES

BY

PRODIP KUMAR MONDAL
ROLL NO: 1655556
SESSION: JULY - 2016

A THESIS SUBMITED TO THE DEPARTMENT OF PHYSICS,
KHULNA UNIVERSITY OF ENGINEERING & TECHNOLOGY,
KHULNA - 9203 IN PARTIAL FULFILMENT OF THE
REQUIRMENT FOR THE DEGREE OF MASTER OF SCIENCE

DEPARTMENT OF PHYSICS
KHULNA UNIVERSITY OF ENGINEERING & TECHNOLOGY
KHULNA - 9203, BANGLADESH
MAY - 2018

TO

MY PARENTS

DECLA RATION

This is to certify that the thesis work entitled as **"Study of the Effect of Rare Earth Ions on the Structural, Magnetic and Electrical Properties of Cu-Zn Ferrites"** has been carried out in partial fulfillment of the requirement for M. Sc. degree in the department of Physics, Khulna University of Engineering & Technology, Khulna - 9203, Bangladesh. The above research work or any part of this work has not been submitted anywhere for the award of any degree or diploma. No other person's work has been used without due acknowledgement.

1. Supervisor — Candidate

---------- ----------

(Prof. Dr. S. S. Sikder) (Prodip Kumar Mondal)

Acknowledgements

I would like to articulate with due respect my sincere and heartiest gratefulness to my respective research supervisor Prof. Dr. Shibendra Shekher Sikder, Department of Physics, Khulna University of Engineering & Technology (KUET) for his indispensable guidance, keen interest, constructive suggestions, fruitful discussion and constant inspiration throughout the research work. It would have not been possible for me to bring out this thesis without his help and constant encouragement

I am indebted to Prof. Dr. Md. Mahbub Alam, Head, Department of Physics, Khulna University of Engineering & Technology (KUET), for his interest and encouragement in my thesis.

It is a matter of great pleasure for me to record the deepest sense of gratitude to Prof. Dr. Abdullah Elias Akther and Prof. Dr. Jolly Sultana, Department of Physics, KUET, have been given me a strong support in various ways during the entire period of my study in the department of Physics KUET. I am thankful to Mr. Alamgir Hossain, Assistant professor, Department of Physics, KUET of his tired less co-operation in my thesis work.

I am grateful to S. Manjura Haque, Head & Chief Scientific Officer, Material Science Division, Atomic Energy Centre, Dhaka, for providing kind opportunity to work her laboratory for experimental work.

My thanks are also for Mr. H. N. Das and Mr. M. A. Mamun, Scientific Officer, MSD, AEC, Dhaka for providing me with technical assistance form time during my research work and providing kind opportunity to work in their laboratory for experimental purpose regarding my thesis.

I am grateful to Mr. Md. Kamrul Hasan Reza, Associate Professor Department of Physics, KUET, Mr. Sujith Kumar Shil, Mr. Suman Halder Assistant Professor, , Mr. Suman Deb nath, Mr. Probal Roy, Mr. Saifullah, Lecture, Department of Physics, KUET for their tireless co-operation in my thesis work. I would also like to thank my well wishers and class fellows Al Masud and Kaushik sarkar.

I am thankful to Eng. F. M Kamal S. E. Dr. Md. Mahbubul Haque S. S. O. of MSD of AECD for providing me with technical assistance from time during my research work at the laboratory of AECD. I am also thankful to Ms. Alhamra Parvin, E.O., Ms. Anjummanara Begum J. E. O., Mr. Anawar Hossain S. S. A. Ms. Nazmunnahar Begum (S.A.-II), Ms. Jarna Begum (S.A.-II) of Material Science Division, Atomic Energy Centre Dhaka (AECD), for their co-operation during the experiments and heartfelt help during the entire period of my research work at the laboratory of AECD.

My special thanks are to the Director, Material Science Division, Atomic Energy Centre Dhaka (AECD) for his kind permission to use the laboratory of Material Science Division, Atomic Energy Centre Dhaka.

A very special thanks to Mrs. Nandita Saha, spouse of Prof. Dr. S. S. Sikder for her heartfelt encouragement, cares and helps throughout the entire period of M. Sc. program. I am greatly indebted to my parents, brother and sisters for their consistent encouragement and inspiration

I also wish to thank the authority of Khulna University of Engineering & Technology (KUET), for providing me with the necessary permission and financial assistance for conducting this thesis work.

Prodip Kumar Mondal

ABSTRACT

Rare earth substituted Fe in Cu-Zn ferrites are well-known technological magnetic materials used for manufacturing of multilayer chip inductor and applications in various electrical devices. The present work is focused on the effect of rare earth ion on structural, magnetic and transport properties of $(Cu_{0.5}Zn_{0.5}Fe_{2-x})RE_xO_4$ [x = 0.00, 0.05 and 0.10] ferrites where RE = La and Sm were prepared by solid state reaction technique keeping in view of their ionic radial and valences for maintain the charge neutrality sintered at 1100^oC with 3 hours holding time. The X-ray diffraction analysis revealed that rare earth free sample shows formulation of single phase cubic spinel structure with no extra peak but other two La and Sm substituted Fe in Cu-Zn samples show additional peaks other cubic spinel structure and corresponding to a second orthoferrite phase. Lattice parameter, bulk density, X-ray density and porosity of the studied samples are increased with both La or Sm substituted ions. Lattice parameter of both series are slightly decrease with increase x content. A significant increase in initial permeability about 620 is found in $(Cu_{0.5}Zn_{0.5}Fe_{1.95})La_{0.05}O_4$ but increase La content decrease initial permeability. This enhancement of permeability may be correlated with improved microstructural features. But the initial permeability decreases with increasing Sm ions in ferrite. Quality factor signifies the merit of the material from the application point of view. The dielectric constant is found to decrease continuously with increasing frequency and remain almost constant at higher frequency range. The dielectric behavior of the experimental ferrite samples explained on the basis of the mechanism of the dielectric polarization and conduction process. The decrease of saturation magnetization with increasing of both rare earth substitutions has been explained on the Neel's collinear two sublattices magnetization model and Yafet-Kittels non-collinear magnetization model.

Contents

CHAPTER-III

EXPERIMENTAL PROCEDURE

CHAPTER-IV
RESULTS AND DISCUSSION

CHAPTER-V
CONCLUSIONS

List of Figures

List of Tables

List of Symbols

Absolute value of admittance = |Y|

Absolute value of impedance = |Z|

Angular frequency = ω

Anisotropy field = H_K

Anisotropy constant = K_l

Average anisotropy = <K>

Bohr magneton = μ_B

Bragg's angle = θ

Bulk density = d_B

Charge of electron = e

Capacitance = C

Coercivity = H_C

Cross-sectional area of toroids = S

Curie temperature = T_C

Dielectric constant = ϵ'

Diffraction angle = θ

Energy per unit area of a 180^{o}Bloch wall = Υ

Exchange integral = J

Exchange coupling constant = J_{ij}

Exchange correlation length = L_O

Face centered cubic = f_{cc}

Frequency = f

Ferromagnetism = FM

Imaginary part of initial permeability = μ''

Impedance = Z

Inductance = L

Initial permeability = μ_i

Inter planner spacing = d

Loss factor = $\tan\delta$

Magnetization = M

Magnetic field = H

Magnetic induction = B

Magneto crystalline anisotropy constant = K_l

Nelson-Riley function = $F(\theta)$

Number of turns = N

Peak temperature = T_P

Permeability of in free space = μ_O

Quality factor = QF

Reactance = X

Real part of initial permeability = μ'

Retentivity = B_r

Remanent ratio	=	M_r
Resistance	=	R
Resistivity	=	ρ
Saturation magnetization	=	M_S
Saturation induction	=	B_S
Saturation polarization	=	J_S
Susceptance	=	B
Susceptibility	=	χ
X-ray density	=	d_X
X-ray diffraction	=	XRD
Yafet-Kittel	=	Y-K
Wavelength	=	λ

INTRODUCTION

1.1 Introduction

The history of ferrite began centuries before the birth of Christ with discovery of stones that attract iron. The most abundant deposits of these stones were found in Asia minor, and hence the name of the materials becomes magnetite (Fe_3O_4).The term ferrite is misused but is commonly used as a class of magnetic oxide compounds that contain iron oxide as a major content[1.1]. Ferrites are magnetic ceramics iron oxides as a major constituent. Soft ferrites, still remain the best magnetic materials and cannot replaced by any other magnetic materials with respect to their very high frequency application because they are inexpensive, most stables, easily manufactured [1.2]. They have wide range of technological application in transformer cores, inductors, high quality filters, radio frequency circuits, rod antenna, read/write heads for high–speed digital tape and operating devices [1.3-1.5]. Ferrites i.e. ferromagnetic cubic spinels are technically important materials. They have been extensively investigated in order to improve good soft magnetic properties. The general combination of such ferrites is MF_2O_4, where M represents one or several of the divalent transition metals such as Mn, Zn, Ni, Co, Cu, Fe or Mg etc. Among the soft ferrites Cu-Zn, Ni-Zn and Mn-Zn ferrites with various additives have enormous technological applications and accordingly extensive research work have been carried out [1.6-1.10].

Ferrimagnetic oxide, ferrite crystallizes with two magnetic sublattices i.e. tetrahedral (A)-site and octahedral (B)-site based on Neel's model. Magnetic and electrical properties of ferrites are strongly dependent on distribution of cation in A- and B-sites and their valence state. It has a distinct class of magnetic materials known as ferromagnetic have spinel structure. They are also called cubic ferrite. Spinel is the most widely used family of ferrite. High values of electrical resistivity and low eddy current losses make them ideal for their use at microwave frequencies. The spinel structure of ferrite as possessed by mineral spinel $MgAl_2O_4$ was first determined by Bragg and Nishikawa in 1915 [1.11-1.12].The spinel ferrites possess properties of both magnetic materials and insulators and are important in many technological applications. Their structural, electrical and magnetic properties depend on magnetic interaction and cations distribution in the two sub-lattices, i.e. tetrahedral (A) and

octahedral (B) sites shown in figure 1.1. The study of spinel ferrites is of great importance from both the fundamental and the applied research point of view. They have many applications in high frequency devices and play a useful role in technological and magnetic applications because of their high electrical resistivity and consequently low magnetic losses over a wide range of frequency. The spinel ferrite unit cell is based on a closed packed oxygen lattice with two types of cations lattice sites: (i) a tetrahedral lattice site A formed by four oxygen anions and (ii) an octahedral lattice site B formed by six oxygen anions.

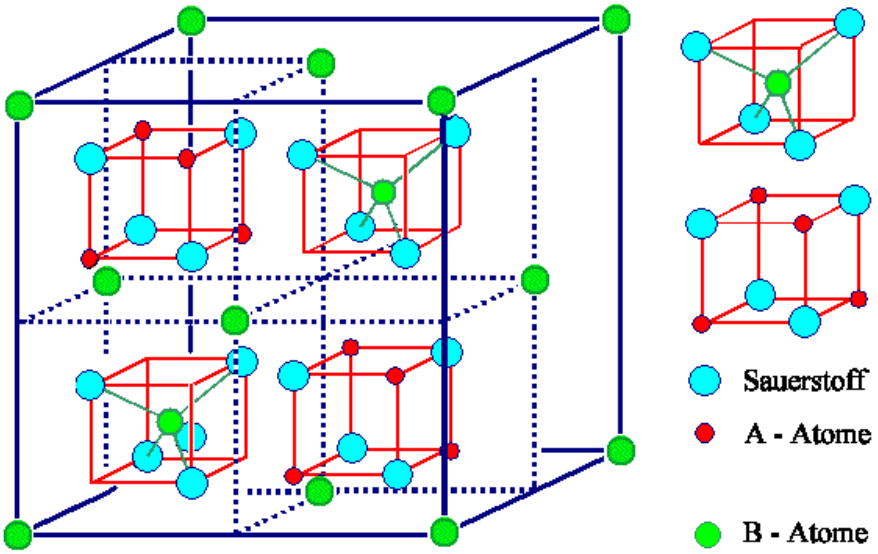

Figure 1.1: The AB_2O_4 spinel structure of ferrites is shown indicating the tetrahedral and octahedral sites.

The interesting physical and magnetic properties of spinel ferrites arise from the ability of these compounds to distribute the cations among the available tetrahedral (A) and octahedral (B) sites [1.13]. The Cu-Zn ferrites are one of the most versatile, reasonable cost magnetic materials for general use in both low and high frequency devices because of their high resistivity, low dielectric losses, mechanical hardness, high Curie temperature and chemical stability. The properties of Cu-Zn ferrites can be tailored with different metals in such as Co^{2+}, Mg^{2+}, Mn^{2+}, Cu^{2+} etc. Amount of liquid phase increase with increasing amount of sintering aids which results in increased densification. However, excessive amount of sintering additives will deteriorate electromagnetic properties of the ferrite. So, optimum content of sintering aids is necessary to achieve good sinter ability as well as better electromagnetic properties.

In addition of small amount of rare earth ions to ferrite samples produces a change in their magnetic and electrical as well as structural properties depending upon the type and the amount of rare earth elements used. Rare earth ions can be divided into two categories. One with radius closes to Fe ions; while the other with the radius larger than Fe ions. If the rare earth ions enter the spinel lattice, the RE-Fe interactions also appears 4f-3d couplings, which can has to changes in the magnetization and Curie temperature (T_c) [1.14]. The rare earth oxides are good electrical insulators and have resistivities at T_c greater than $10^6\Omega$-cm [1.15]. Reslescu *et al.* [1.16] investigated the effect of Fe replacement by RE [Yb, Eu, Sm, Tb, Gd, Dy and Ce] ions on the properties of $(Ni_{0.7}Zn_{0.3})Fe_2O_4$ ferrite. The results showed that the electrical resistivity of ferrite increased by substituting a small quantity of Fe_2O_3 with RE_2O_3. Rare ion forms the orthoferrite phase. The occupation of RE ions on B-sites impedes the motion Fe^{2+} in conduction process in ferrite. Effect of RE substitution by Gd, La, Eu and Y on the structure, magnetic and electrical properties of Ni-Zn ferrites was found that the relative density of sintered bodies decreased the initial permeability and magnetic loss tangent which could be explained by a combination of low density, small grain size, secondary phase formation and more lattice defects [1.17-1.18].

The most effective sintering Cu-Zn ferrite the systematic research is still necessary for effect has been undertaken to produce Cu-Zn ferrite doped with Sm_2O_3 and La_2O_3. The polycrystalline Cu-Zn ferrite could be considered as the most versatile ferrites, due to their several advantages over others ferrites such as low cost of raw materials, low density, and high operating frequency range is one of the soft ferrites used in electronic and magnetic devices such as transformers, inductors and magnetic heads for high frequency because their electrical resistivity is higher than those of the soft magnetic alloys. To carry out on the influence of different rare earth atoms on the properties like high saturation magnetization, high permeability, high resistivity, dielectrics etc. The systematic research is still necessary for a more comprehensive understanding and properties of such materials.

1.2 The Aims and Objectives of the Present Work

The effect of rare earth ions on the structural, magnetic and transport properties of $(Cu_{0.5}Zn_{0.5}Fe_{2-x})RE_XO_4$ ferrites where RE = La and Sm. Rare earth ion formed orthoferrite ($REFe_2O_4$) phase and the formation of these secondary phases in

ferrite during sintering process was governed by the type and the amount of RE^{3+}ion used.

The main objectives of the present research work are made as follows:

(i) $(Cu_{0.5}Zn_{0.5}Fe_{2-x})La_XO_4$ [x = 0.00, 0.05 & 0.10]

(ii) $(Cu_{0.5}Zn_{0.5}Fe_{2-x})Sm_XO_4$ [x = 0.00, 0.05 & 0.10]

The raw oxide materials in the synthesis of ferrites samples are commercially available of nano particle size of 20- 70nm. It is ferromagnetic in nature and posses a cubic structure and can be used in various electromagnetic devices due to their high resistivity and high frequency tolerance. At present, Bangladesh is totally dependent upon the imported ferrite cores and other soft magnetic materials. If we can develop rare earth doped ferrites in our country that may alleviate present problems of our country.

- To synthesis a series of $(Cu_{0.5}Zn_{0.5}Fe_{2-x})RE_XO_4$ in which RE = La and Sm.
- To investigate the structure of the composition using XRD.
- To study electrical and magnetic properties of the sample using LCR meter, VSM.
- To study effect of La^{3+} and Sm^{3+}substitution for Fe^{3+} on structural and transport properties of the optimized Cu-Zn ferrite.
- Optimize the concentration of rare earth doped for the best magnetic and transport properties.

Finally, it is expected to use powder particles as starting materials may give uniform microstructure exhibiting better magnetic and electrical transport properties. With the substitution of rare earth metals in the Cu-Zn ferrite system permeability and magnetic properties are expected to be improved. The accumulated results would be interpreted on the basis of existing theories of magnetism.

1.3 Experimental Reason for This Research Work

Polycrystalline rare earth ferrites have been prepared by standard solid state reaction techniques. High purity powders of CuO (99.9%), ZnO (99.9%), Fe_2O_3 (99.9%), La_2O_3(99.9%) and Sm_2O_3(99.9%) has been mixed thoroughly in an appropriate amount mixing will be performed in both dry and acetone. The mixed powders have been calcined at high temperature. After calcinations toroid and disk shaped sample has been prepared and has been sintered at various temperatures. The experimental methods that have been used in this work are as follows:

- The prepared sample has been characterized in terms of their crystal structure, unit cell parameters and phase presents in the prepared samples with the help of X-ray diffractometer (XRD).
- Sintering of the samples has been carried out in a microprocessor controlled high temperature furnace.
- Permeability, magnetic loss factor and relative quality factor as a function of frequency and temperature has been determined using an impedance analyzer.
- Dielectric properties as a function of frequency and temperature have been determined using an impedance analyzer.
- Magnetization of the samples has been measured as a function of field using vibrating sample magnetometer (VSM).

1.4 Application of Ferrites

Ferrites are primarily used as inductive components in a large variety of electronic circuits such as low noise amplifiers, filters, voltage controlled oscillators, impedance matching networks for instance. The basic components to produce the inductance are very soft ferrite and a metallic coil. Multilayer chip inductors for high frequency circuit's applications use sheets made of dielectric ceramics instead of ferrite industry. Ferrites are used widely due to their following applications.

(i) Ferrites are part of low power and high flux transformers which are used in television.

(ii) Small antennas are made by winding a coil on ferrite rod used in transistor radio receiver

(iii) In computer, non volatile memories are made of ferrite materials. They store in formation even if power supply fails. Non-volatile memories are made up of ferrite materials as they are highly stable against severe shock and vibrations.

(iv) Ferrites are used in microwave devices like circulators, isolators, switch phase shifters and in radar circuits.

(v) Ferrites are used in high frequency transformer core and computer memories i.e. computer hard disk, floppy disks, credit cards, audio cassettes, video cassettes and recorder heads.

(vi) Ferrites are used to produce low frequency ultrasonic waves by magnetostriction.

(vii) Nickel alloys are used in high frequency equipments like high speed relays, wideband transformers and inductors. They are used to manufacture transformers, inductors, small motors, synchros and relays. They are used for precision voltage and current transformers and inductive potentiometers.

(viii) They are used as electromagnetic wave absorbers at low dielectric values.

(ix) Ferrites are important components for the latest products, such as cellular phones, video cameras, note book computers, hard temperatures and floppy drives.

(x) Ferrites for the applications in producing multilayer-type chips mainly because these oxide

1.5 Review of the Earlier Research Work

A ferrite is a type of ceramic compound composed of iron (III) oxide (Fe_2O_3) combined chemically with one or more additional metallic elements [1.19]. They are both electrically nonconductive and ferromagnetic, meaning they can be magnetized or attracted to a magnet. Ferrite is a body-centered cubic (BCC) form of iron, in which a very small amount (a maximum of 0.02% at 1333°F / 723°C) of carbon is dissolved [1.20].Among the soft magnetic materials, polycrystalline ferrites have received special attention due to their magnetic properties and high electrical resistivity over a wide range of frequencies; starting from a few hundred Hz to several GHz. Spinel type ferrites are commonly used in electric and magnetic devices due to their high magnetic permeability and low magnetic loses [1.21 -1.22] and also used in electrode materials for high temperatures applications because of their high electrical resistivity. Many investigators have focused their attention on the improvement of electromagnetic properties of the ferrite by divalent ions substitution. Generally the divalent metal ions (M^{2+});Ni, Zn, Cu, Mg, Mn, Co or mixtures of these are substituted in different spinel ferrites.

The studies on microstructure and composition related magnetic properties have been reported for Cu-Zn ferrites by several researchers, which are also given below:

Khan *et. al* [1.23] and Low *et. al* [1.24] reported that Ni-Cu-Zn ferrites are well established soft magnetic material for MLCI applications because of their relatively low sintering temperature, high permeability in the RF frequency region and

high electrical resistivity. Khan *et. al* [1.9] studied complex permeability spectra of Ni-Cu-Zn ferrites. The particle size increase the sintering temperature is raised. For the composition and different sintering temperature was found that the real permeability in that low frequency region decreases CuO.

Hossain M. A. *et. al* [1.25 - 1.26] introducing optimally rare earth materials in to the ferrite specimen like Ni-Zn ferrites it is possible to develop good magnetic materials. Rare earth Y^{3+} and Eu^{3+} ions replace the metallic cations in tetrahedral A-sites or octahedral B-sites to improve various properties of the samples. Introducing a very poor amount of rare earth ions may significantly changes the microstructure, electrical, magnetic as well as optical properties of the ferrites composites.

Martin Šoka *et al.*[1.22] analyzed the Magnetic Properties of Rare-Earth (RE) Substituted Nickel Zinc Ferrites and Investigated that small RE additives play an important role in modification of the structure and intrinsic/extrinsic magnetic properties of ferrites due to the magneto-crystalline anisotropy in the RE-doped compounds and the RE-Fe interaction. They noticed the significant changes of the investigated properties. Curie temperature and coercivity increase with substitution, meanwhile susceptibility, remanent magnetic flux density, and saturation magnetic flux density decreases. In addition, complex permeability spectra analysis revealed the shift of critical frequencies to higher values.

Costa *et. al.* [1.27] investigated the effect of Sm on the microstructure, relative density and magnetic properties of $(Ni_{0.5}Zn_{0.5})Sm_x\ Fe_{2-x}O_4$ ferrites. Results showed that the increased relative density and decreased average grain size with rare earth substitutions. It also showed that the increase in coercive field and decrease in permeability with rare earth substitution and show a bi-phasic microstructure constituted of a matrix of dark grains and a second phase ($SmFeO_3$).

Roy *et. al.* [1.28-1.29] reported the impact of La^{3+} and Sm^{3+} substitution showed improved resistivity Ni-Cu-Zn ferrites. They also discussed relative density and grain size of ferrites increased with increase Sm^{3+} substitution. Increased densification may be due to the appearance of excess Ni, Zn and Cu composed with Fe in the composition. A significant increase in μ_i of the ferrites was found at small fraction of Sm^{3+} substitution about 0.05. Similarly this substitution may improve the electromagnetic properties in ferrites.

Sun et al. [1.30] investigated the effects of rare earth ions on the properties of $(Ni_{0.5}Zn_{0.5})Fe_{1.98}RE_{0.02}O_4$ (RE = Y, Eu or Gd) nominal compositions. The partial

substitution of Fe^{3+} with a small amount of RE ions increased the electrical resistivity and relative loss factor, whereas, it slightly decreased the T_c. Rezlescu et al. [1.31] investigated the influence of rare earth ions like Yb, Er, Dy, Tb, Gd, Sm substitution on structure, magnetic and electrical properties of $(Li_{0.3}Zn_{0.4})Fe_{1.96}RE_{0.04}O_4$ ferrites. They found that RE_2O_3 facilities the formation of secondary phases at grain boundary which suppressed the grain growth and results are showed that the T_c shifted to lower temperature and increased the electrical resistivity.

Jacobo et. al. [1.32] worked on $(Ni_{0.5}Zn_{0.5})Fe_{1.98}RE_{0.02}O_4$ ferrites, with RE = Y, Eu and Gd. The results showed a small increase in the hyperfine field parameters and a strong decrease of the total resonant area with respect to the pure Ni-Zn ferrite. T_c decreases and coercive fields increased with substitution rare earth ions. By adding much large ionic radii rare earth ions resulted in local distortion and disorder, enough to induce a softening of the network.

In the present work the addition of rare earth ion with replace Fe ions as sintering aid will reduce the sintering temperature which may affect to obtain homogeneous microstructure and enhance electrical and magnetic properties. With the substitution of rare earth metals in the Cu-Zn ferrite system permeability and magnetic properties are expected to be improved.

1.6 Summary of the Thesis

Chapter 1: Deals with definition, research background, and importance's of ferrite, application of ferrite as well as objective of the present work.

Chapter 2: Brief overviews of the materials, theoretical background, characterizations, magnetism and crystal structure of the spinel ferrite have been described here.

Chapter 3 Describes the methodology of ferrite preparation and its modification and this chapter illustrated with the experimental theory and technique which were taken to account the structural, electrical and magnetic properties of ferrite.

Chapter 4 Results and discussion are thoroughly explained. The various experimental and theoretical studies namely effect rare earth metal substitution on the structural, electrical and magnetic properties of Cu-Zn ferrites are presented and a brief discussion has been given here.

Chapter 5 This chapter included the conclusion and the outcome of the thesis.

References are added at the end of each chapter.

THEORETICAL BACKGROUND

2.1 Rare Earth Ferrites

Ferrites have been studies since 1936. They have an enormous impact over the application of magnetic materials. Ferrites are essentially ceramic materials, compound of iron, boron, barium, strontium, lead, zinc, magnesium or manganese. The ingredients are mixed, preferred, milled/crushed, dried, shaped and finally pressed and fired into their final hand a brittle state. Now a days newer family of ferrite materials have been discovered, which are rare-earth types. Influence of rare earths substituted different ferrites are becoming the promising materials for different properties. Rare earth ions can improve densification and increase permeability and resistivity. Addition of small amount of rare earth ions to ferrite samples producing a change in their magnetic and electrical as well as structural properties depending upon the types and the amount of rare earth elements used.

The rare earth elements are all metals, and the group is often referred to as the "rare earth metals." These metals have many similar properties and that often causes them to be found together in geologic deposits. They are also referred to as "rare earth oxides" because many of them are typically sold as oxide compounds. Rare earth elements are not as "rare" as their name implies. Thulium and lutetium are the two least abundant rare earth elements - but they each have an average crustal abundance that is nearly 200 times greater than the crustal abundance of gold [2.1]. However, these metals are very difficult to mine because it is unusual to find them in concentrations high enough for economical extraction. The most abundant rare earth elements are cerium, yttrium, lanthanum and neodymium [2.2].

They have average crustal abundances that are similar to commonly used industrial metals such as chromium, nickel, zinc, molybdenum, tin, tungsten and lead [2.1]. Again, they are rarely found in extractable concentrations. The rare earth ions can be divided into two categories; one with the radius closes to Fe ions; while the other with ionic radius larger than Fe ions [2.3].The difference in their ionic radii will lead to micro strains, which may cause domain wall motion resulting in deformation of the spinel structure. It has been stated that ions commonly reside at the octahedral sites by replacing Fe^{3+} ions and have limited solubility in the spinel lattices due to their large ionic radii [2.4]. The rare earth ions have unpaired 4f electrons and the strong spin orbit coupling of the angular momentum.

Moreover, 4f shell of rare earth ions is shielded by $5S^2$ $5P^6$ and almost not affected by the potential field of surrounding ions. Doping rare earth ions into spinel type ferrites, the occurrence of 4f-3d couplings which determine the magneto-crystalline anisotropy in spinel ferrite can also improve the electric and magnetic properties of spinal ferrites [2.5-2.8]. Spinel ferrites ceramic are widely used in microwave devices to control transmission path, frequency, amplitude and phase of microwave signals. Accurate dielectric and magnetic properties measurement at the operational frequency and temperature ranges are needed for optimized development of these devices, as well as to assist in the manufacture of the ferrite [2.9]. The structured magnetic materials have an interesting area of study because of its possible applications in a variety of widely areas ranging from information technology to biotechnology [2.10]. The properties of ferrites are being improved due to the increasing trends in ferrite technology. It is believed that there is a bright future for ferrite technology. Cu-Zn ferrite doped with rare earth metals like Sm_2O_3 and La_2O_3 are used to study the effect of enhancing the magnetic properties. Therefore, hard ferrites constitute the major fraction since they are used whether energy per unit eight and cost are important considerations [2.11]. Ferrite are a class of chemical compounds with the formula AB_2O_4 where A and B represent various metal cations usually including iron. These ceramic materials are used in applications ranging from magnetic components in micro electronics.

2.2 Ferrites

Ferrites are complex magnetic oxides that contain the ferric oxide (Fe_2O_3) and their basic magnetic component [2.12]. They are both electrically nonconductive and ferrimagnetic, meaning they can be magnetized or attracted to a magnet. On the other hand ferrites are a class of ferrimagnetic ceramic chemical compounds consisting of mixtures of various metal oxides, usually including iron oxides.

2.2.1 Classification of Ferrites and its Relevance

Ferrites are essentially ceramic materials, compound of iron, boron, barium, strontium, lead, zinc, magnesium or manganese. The ingredients are mixed, preferred, milled / crushed, dried, shaped and finally pressed and fired into their final hand in brittle state. Now a days newer family of ferrite materials have been discovered, which are rare-earth types. Additives of rare earth metals like lanthanum oxide are

used to study the effect of enhancing the magnetic properties. They are primarily used as permanent magnets. These ferrites are very stable with the excellent characteristic of high resistivity. Ferrites are classified into two categories based on their coercive field strength. They are:

(i) Soft ferrite with coercive field strength < 10 Oe

(ii) Hard ferrite with coercive field strength > 125Oe

According to crystallographic structures ferrites can be classified into three different types [2.13]

(i) Spinel ferrites (Cubic ferrites)

(ii) Hexagonal ferrites

(iii) Garnets

2.2.2 Spinel Ferrite

Ferrite material is so much popular as spinel compound. In general, spinel ferrites show low magnetic anisotropy i.e., dependence of magnetization on crystallographic directions, and are magnetically soft i.e. show low coercive fields. Exceptions could be co-containing ferrites which are not only strongly magnetically anisotropic but also show large coercive fields strength.

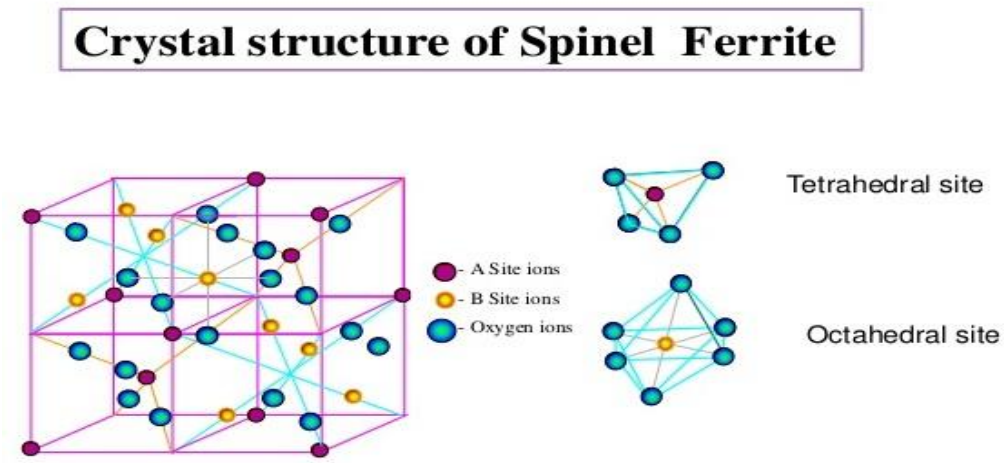

Figure 2.1: Crystal structure of spinel ferrite

These materials also exhibit a ferromagnetic material like hysteresis loop when placed in a varying magnetic field. Many magnetic oxides, Fe_3O_4 and $CuFe_2O_4$ are spinels. Cubic spinel ferrites have a formula AB_2O_4 which crystallize with a face centered cubic structure. In these structures, two cations occupy tetrahedral and octahedral sites in an FCC lattice made by O (Oxygen) atoms. One unit cell consists of eight formula units of AB_2O_4 hence containing a total of 32 octahedral interstices

with one fourth occupancy and 64 tetrahedral interstices with one eight occupancy by the cations [2.14]. Because of having the combination of two different types of ions, the structure refers to point out as spinel. Normal spinel structures are usually cubic close-packed oxides with one octahedral and two tetrahedral sites per formula unit. The tetrahedral spaces are smaller than the octahedral spaces. B^{3+} ions occupy half the octahedral holes, while A^{2+}ions occupy one-eighth of the tetrahedral holes.

2.2.3 Hexagonal Ferrites

This was first identified by Went, Rathenau, Gorter and Van Ostershout 1952 [2.15] and Jonker, Wijn and Braun 1956. Hexa ferrites are hexagonal or rhombohedral ferromagnetic oxides with formula $MFe_{12}O_{19}$, where M is an element like Barium, Lead or Strontium. The third type o ferrites are often called the barium ferrites. These compound usually cation BaO, in addition to Fe_2O_3, as the basic component oxide are also known as magneto plumbites.

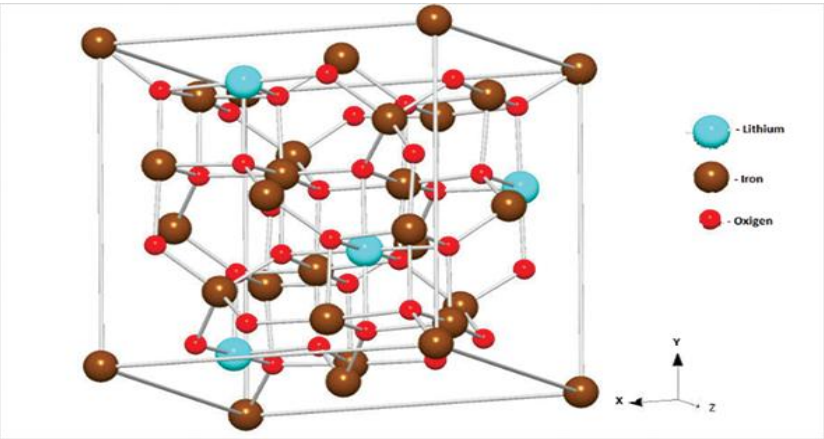

Figure 2.2: Crystal structure of hexagonal ferrite

The common chemical formula of barium ferrites is l (BaO).m (MO).N $(Fe_2O_3)_n$ or Ba^{3+} .Mm^{2+} Fe_{2n}^{3+} O^{2-}_{1+m+3n} , where l is much more complex than the previous two in both in terms of composition of barium ferrites may be complex than the previous two in both in terms of composition of barium ferrites may be changed one is to vary the M^{3+} ions. Mg, Mn, Fe, Co, Ni, Cu and Zn are found suitable for the formation of hexagonal ferrites. Another way to alter the values of l, m and n. Basic compositions are found at 1-0-6(M), 1-2-8 (M_2W), 2-2-6 (M_2Y) and 3-2-12($M_2\rightarrow$). In these ferrites, oxygen ions have closed packed hexagonal crystal structure. They are widely used as permanent magnets and have high coercivity. They are used at very high frequency. Their hexagonal ferrite lattices are similar to the spinel structure with

closely packed oxygen ions, but there are also metal ions at some layers with the same ionic radii as that of oxygen ions. Hexagonal ferrites have larger ions than that of garnet ferrite and are formed by the replacement of oxygen ions. Most of these larger ions are barium, strontium or lead.

2.2.4 Garnet

Garnets are usually known as minerals. In the context of magnetic materials, garnets are represented by a general formula $Y_3Fe_5O_{12}$, containing two magnetic ions, one typically being iron and another being rare earth. Here R, in addition to yttrium can be one of lanthanide atoms such as lanthanum, cerium, samarium etc. The unit cell of $Y_3Fe_5O_{12}$is cubic and contains 8 formula units i.e. 160 atoms, quite complex! In garnet ferrites, orbital magnetic contribution of iron atoms is quenched due to shielding from crystal field while lanthanide ions contribute to both orbital and spin magnetic moment, thus contributing more to the total magnetic moment. Garnets can be quite useful materials in microwave applications because of their high electrical resistivity and hence lower losses around microwave frequencies. The material is also easy to synthesize in either of bulk polycrystalline ceramic, single crystal or thin film forms. The structural parameters as well as magnetic properties can be tuned by tailoring the composition of the material [2.16].

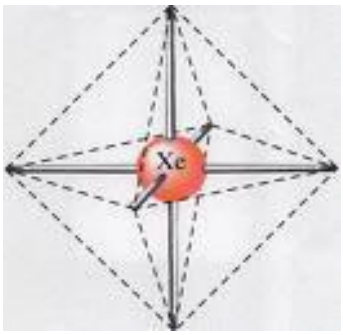

Figure 2.3: Cubic ferrite of garnet

The present research work is on spinal ferrites therefore it has been discussed in detail the spinel ferrites only.

2.3 Types of Spinel Ferrites

The spinel ferrites have been classified into three categories due to the distribution of cations on tetrahedral (A) and Octahedral (B) sites.

(i) Normal spinel ferrites

(ii) Inverse spinel ferrites

(iii) Intermediate or Mixed spinel ferrites.

2.3.1 Cation Distribution in Spinels

The cation distribution in the spinel $Me^{2+}Me^{3+}O_4$ can be as follows

- **Normal**

The Me^{2+} cations are in tetrahedral positions, while the two Me^{3+} cations are in octahedral sites.The square brackets are generally used to present the octahedral sites,i.e. $Me^{2+}[Me^{3+}]O_4$

- **Inverse**

In the case the Me^{2+} cation and one of the Me^{3+} cations are in octahedral positions while the second Me^{3+} cation occupies a tetrahedral positions.The arrangement is as $.Me^{3+}[Me^{2+}Me^{3+}]O_4$.

- **Intermediate**

The arrangement of the form like $Me^{3+}_{1-\delta} Me^{2+}_{\delta} [Me^{3+}_{1-\delta} Me^{2+}_{1+\delta}]O_4$ is often reffered as intermediate, where δ is called the inversion parameter. $\delta = 0.0$ for completely normal and $\delta = 1.0$ for completely inverse spinels and $0<\delta<1$ for intermediate spinels. [2.17 - 2.18]

The factors affecting the cation distribution over A and B sites are as follows:

(i) The size of the cations

(ii) The electronic configuration of cations

(iii) The electronic energy

(iv) The saturation magnetization of the lattice

Smaller cations (trivalent ions) prefer to occupy the A-sites. The cations have special preference for A and B sites and the preference depends on the following factors:

(i) Ionic radius

(ii) Size of interstices

(iii) Sintering temperature and

(iv) Orbital preference for the specific coordination.

The preference of cations is according to Verway- Heilmar scheme [2.19]

(i) Ions with strong preference for A-sites Zn^{2+}, Cd^{2+}, Ga^{2+}, In^{3+}, Ge^{4+}.

(ii) Ions with strong preference for B-sites Ni^{2+}, Cr^{3+}, Ti^{4+}, Sn^{4+}.

(iii) Indifferent ions are Mg^{2+}, Al^{3+}, Fe^{2+}, Co^{2+}, Mn^{2+}, Fe^{3+}, Cu^{2+}.

Moreover the electrostatic energy also affects the cation distribution in the spinel lattice. The cations of the smallest positive charge reside on the B-sites having six anions in surrounding i.e. the most favorable electrostatic conduction.

2.4 Types of Ferrites with Respect to Hardness

. The wide variety of magnetic materials can be divided into two groups, the magnetically soft and the magnetically hard. Soft magnetic materials are those materials that are easily magnetized and demagnetized. They have low magneto crystalline anisotropy resulting in reduced coercivity and high permeability. They typically have intrinsic coercivity less than 1000 Am^{-1}. They are used primarily to enhance and/or channel the flux produced by an electric current. The important parameter, often used as a figure of merit for soft magnetic materials, is the high relative permeability. The other main parameters of interest are the coercivity, the saturation magnetization and the electrical conductivity.

The main consideration for material selection is most likely to be the permeability. For example, in shielding applications the flux must be channeled through the material. Where the material is used to generate a magnetic field or to create a force then the saturation magnetization may also be significant. The important consideration is how much energy is lost in the system as the material is cycled around its hysteresis loop. The energy loss can originate from three different sources:

(i) Hysteresis loss, which is related to the area contained within the hysteresis loop

(ii) Eddy current loss, which is related to the generation of electric current in the magnetic material and the associated resistive losses and

(iii) Anomalous loss, which is related to movement of domain walls within the material.

Hysteresis losses can be reduced by the reduction of the coercivity, with a consequent reduction in the area contained within the hysteresis loop. Eddy current losses can be reduced by decreasing the electrical conductivity and is important by the laminating the material, which on influence on overall conductivity and is important because of skin effects at higher frequency. Finally, anomalous losses can be reduced, within which there will be no hindrance to the motion of domain walls.

2.4.1 Soft Ferrites

At high frequency metallic soft magnetic materials simply cannot be used due to the eddy current losses. Therefore soft ferrite, which is ceramic insulators, becomes the most desirable material. These materials are ferrimagnetic with a cubic crystal structure and the general composition $MO.Fe_2O_3$ where M is a transition metal such as nickel, manganese, magnesium, zinc, cobalt or cadmium. The magnetically soft ferrites first came into commercial production in 1948. Mn -Zn ferrite sold commercially as ferroxcube, can be used at frequencies up to 10MHz, for example in telephone signal transmitters and receivers and in switch mode power supplies. For these type of application the driving force to increase frequency is to allow miniaturization

Additionally, parts of the family of soft ferrites are the microwave ferrites e.g. Yttrium iron garnet .These ferrite are used in the frequency range from 100 MHz to 500GHz. For waveguides, for electromagnetic radiation, and in microwave device such as phase shifters. Application of soft ferrite include: cores for electro-magnets, electric motors, transformers, generators, and other electrical equipment.

2.4.2 Hard Ferrites

Hard ferrites are difficult to magnetized or demagnetized. Hard magnets are characterized by high remanent inductions and high coercivities. The higher coercivity means the materials are very resistant to becoming demagnetized an essential characteristic for a permanent magnet. They also conduct magnetic flux will and have a high magnetic permeability. This enables these so-called ceramic magnets to store stronger magnetic fields than iron itself. They are cheap and are widely used in household products such as refrigerator magnets. They generally exhibit large hysteresis losses. Hard ferrite referred to as permanent magnets retain their magnetism after being magnetized.

Hard ferrite likes Ba-ferrite, Sr-ferrite, Pb-ferrite are used in communication device operating with high frequency currents because of their high resistivity, negligible eddy currents and lower loss of energy due to Joule heating and hysteresis. These are found useful in many applications including fractional horse-power motors, automobiles, audio- and video-recorders, earphones, computer peripherals, and clocks.

2.5 Magnetic Exchange Interaction

In physics, the exchange interaction is a quantum mechanical effect without classical analogue which increases or decreases the expectation value of the energy or distance between two or more identical particles when their wave functions overlap. For example, the exchange interaction results in identical particles with specially symmetric wave function (bosons) appearing closer together than would be expected distinguishable particles, and identical particles with spatially anti symmetric wave functions (fermions) appearing further apart. The exchange interaction is the mechanism responsible for ferromagnetism, among other consequences.

The electron spin of the two atoms Si and Sj which is proportional to their product .The exchange energy can be written as universally in terms of Heisenberg Hemiltonian [2.20]

$$H = -\Sigma J_{ij}\, S_i.S_j = -\Sigma J_{ij}\, S_i\, S_j \cos\varphi, \qquad (2.1)$$

Where J_{ij} is the exchange integral represents the strength of the coupling between the spin angular momentum i and j and φ is the angle between the spins. It is well known that the favored situation is the one with the lowest energy and it turns out that there are two ways in which the wave functions can combine there are two possibilities for lowering the energy by H.

These are:

(i) If J_{ij} is positive and the parallel spin configuration ($\cos\varphi = 1$) the energy is minimum.

(ii) If J_{ij} is negative and the spins are antiparallel ($\cos\varphi = -1$) energy is maximum. This situation leads to antiferromagnetism.

2.5.1 Electron spin

Spin is an intrinsic form of angular momentum carried by elementary particles, composite particles (hadrons), and atomic nuclei [2.21 - 2.22]. The electron behaves as if it were spinning about an axis, thereby generating a magnetic field whose direction depends on the direction of spin. The two directions for the magnetic field correspond to the two possible values for the spin quantum number, m_s.

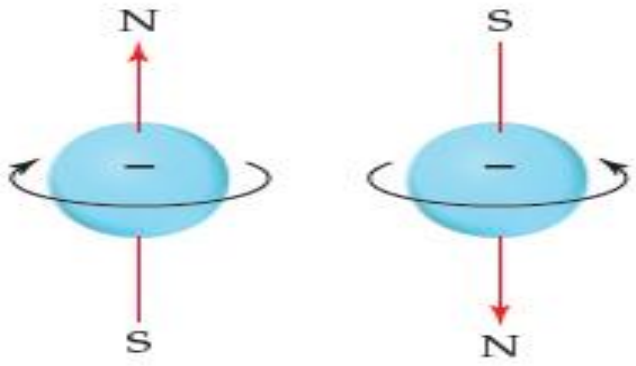

Figure 2.4: Electron Spin

From this figure can say:

- There are only two possible values for the spin quantum number because an electron can move only in 2 directions: up and down.
- There are only two possible values for the spin quantum number because an electron can move only in 2 directions: left and right.
- There are only two possible values for the spin quantum number because an electron can spin only in 2 directions: clockwise and anticlockwise.

2.5.2 Magnetization Process

A review of the magnetization process, namely the response of ferro-(ferri) magnetic material (bulk) to an applied field with a semi-microscopic approach is presented. In Ferro-or ferri-magnetic material, the magnetization curves, especially in low magnetic fields differ widely from sample to sample and as a function of the magnetic history of the sample i.e., of the previous fields which have been successively applied.

2.5.3 Magnetization Curve

For unmagnetized bulk materials, there is a zero net magnetic moment. It can be predicted that there will be an infinite number of degree of magnetization between the unmagnetized and saturation conditions, when the material is subjected to an external magnetic field. These extreme situations are corresponds respectively to random orientation of domains complete alignment is one direction with elimination of domain walls. If we start with a demagnetized specimen and increase the applied magnetic field, the bulk material will progressively magnetized by the domain dynamics. The magnetization of the sample will follow the course as shown in figure

2.7 [2.23]. The slop from the origin to a point on the curve r the ratio $\frac{M}{H}$ is defined as magnetic susceptibility. This curve is called magnetization curve. This curve is generally perceived as being made of three major portions.

The first, the lower section, is the initial susceptibility region and characterized by reversible domain wall movements and rotations. By reversible means that after the magnetization slightly with an increase in field the origin magnetization can be reversed if the field is reduced to initial value. The condition of the displacement walls to an initial permeability is entirely dependent on the sort of material studied. In the second stage magnetization curve if the field is increased, the intensity of the magnetization increases more drastically is called the irreversible magnetization range. This range is obtained mainly by the reversible domain wall motion from one stable state to another.

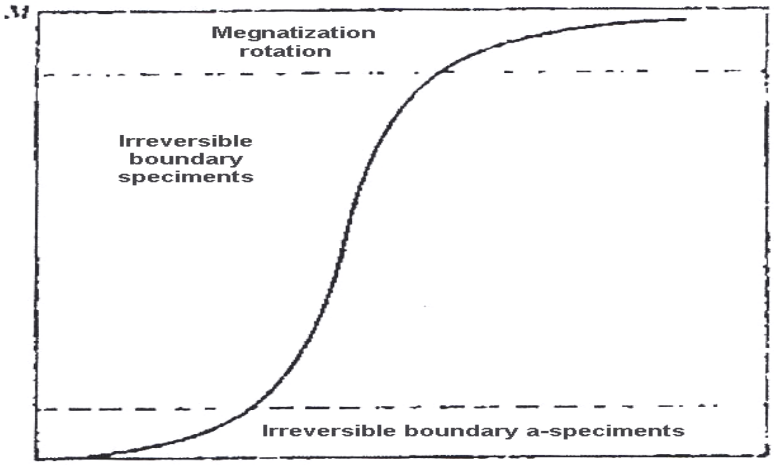

Figure 2.5 Domain dynamics during various parts of the magnetization curve

2.5.4 Magnetic Hysteresis Loop

The magnetic hysteresis loop above shows the behavior of a ferromagnetic core graphically as the relationship between B and H is non-linear. Starting with an unmagnetised core both B and H will be at zero, point 0 on the magnetization curve. If the magnetization current, i is increased in a positive direction to some value the magnetic field strength H increases linearly with i and the flux density B will also increase as shown by the curve from point 0 to point a as it heads towards saturation. Now if the magnetizing current in the coil is reduced to zero, the magnetic field circulating around the core also reduces to zero. However, the coils magnetic flux will

not reach zero due to the residual magnetism present within the core and this is shown on the curve from point a to point b.

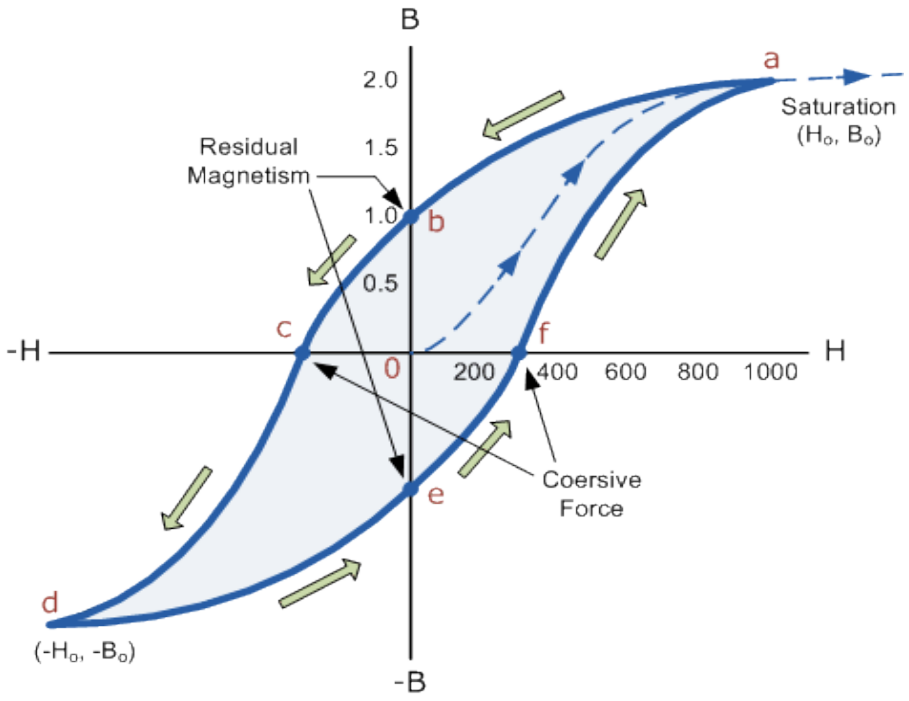

Figure 2.6 Magnetization hysteresis curve

To reduce the flux density at point b to zero we need to reverse the current flowing through the coil. The magnetizing force which must be applied to null the residual flux density is called a “Coercive Force”. This coercive force reverses the magnetic field re-arranging the molecular magnets until the core becomes unmagnetised at point c. An increase in this reverse current causes the core to be magnetized in the opposite direction and increasing this magnetization current further will cause the core to reach its saturation point but in the opposite direction, point d on the curve. This point is symmetrical to point b. If the magnetizing current is reduced again to zero the residual magnetism present in the core will be equal to the previous value but in reverse at point e.

Again reversing the magnetizing current flowing through the coil this time into a positive direction will cause the magnetic flux to reach zero, point f on the curve and as before increasing the magnetization current further in a positive direction will cause the core to reach saturation at point a. Then the B-H curve follows the path of a-b-c-d-e-f-a as the magnetizing current flowing through the coil alternates between a positive and negative value such as the cycle of an AC voltage. This path is called **a** magnetic hysteresis loop shown in figure 2.6.

2.6 Theory of Initial Permeability

Permeability is namely defines as the proportional constant between the magnetic field induction B and applied intensity H:

$$B = \mu H \tag{2.2}$$

If a magnetic material is subjected to an AC magnetic field as given below:

$$H = H_0 e^{i\omega t} \tag{2.3}$$

Then it is observed that the magnetic flux density B experiences a delay. The delay is caused due to presence of various losses and is thus expressed as

$$B = B_0 e^{i(\omega t - \delta)} \tag{2.4}$$

where δ is the phase angle and marks the delay of B with respect to H. The permeability is then given by

$$\mu = \frac{B}{H} = \frac{B_0 e^{i(\omega t - \delta)}}{H_0 e^{i\omega t}} \tag{2.5}$$

$$= \frac{B_0 e^{-i\delta}}{H_0} = \mu' - i\mu'' \tag{2.6}$$

$$\text{Where} \quad \mu' = \frac{B_0}{H_0}\cos\delta \tag{2.7}$$

$$\mu'' = \frac{B_0}{H_0}\sin\delta \tag{2.8}$$

The real Part μ’ of complex permeability μ as expressed in equation (2.6) represent the component of B which is in phase with H, so it corresponds to the normal permeability. If there is no losses , we should have μ = μ', The imaging part μ" corresponds to the part of B which is delayed by phase angle arranging up to 90° from H . The presence of such a component requires a supply of energy to maintain the alternating magnetization regardless of the origin of delay.

The ratio of μ" to μ' gives

$$\frac{\mu'}{\mu''} = \frac{\frac{B_0}{H_0}\sin\delta}{\frac{B_0}{H_0}\cos\delta} = \tan\delta \tag{2.9}$$

This tan δ is called the loss Factor or loss tangent. The Q-Factor or quality factor is defined as the reciprocal of this loss factor, i.e

$$Q = \frac{1}{\tan\delta} \tag{2.10}$$

EXPERIMENTAL PROCEDURE

3.1 Methodology of Rare Earth Ferrite Preparation

The preparation of rare earth ferrites with optimum desired properties is still a complex and difficult task. Knowledge and control of the chemical composition, homogeneity and microstructure are very crucial. The rare earth ferrite is not completely defined by its chemistry and crystal structure but also requires knowledge and control of parameters of its microstructure such as density grain size, porosity and their intra and intergranular distribution. It is well known that almost all rare earth ferrites decompose at the elevated temperature of we want to melt them under normal conditions. This happens because the oxygen splits off at higher temperature reducing Fe^{3+} and Fe^{2+}. This necessarily implies that ferrite preparation by melting as in case of metals is not possible. The normal methods of preparation of ferrites comprise of the conventional ceramic method or powder metallurgy chemical co-precipitation method and sol-gel method.

In this work conventional ceramic method has been employed for the preparation of $(Cu_{0.5}Zn_{0.5}Fe_{2-x})RE_xO_4$ ferrites for its relative simplicity and availability. The excellent powder preparation process and sintering facility available at the Solid State Laboratory, Khulna University of Engineering & Technology, Khulna, has been utilized for the preparation of samples.

3.1.1 Compositions of the Studied Ferrites

A series of mixed ferrites of various compositions were prepared by solid state reaction technique keeping in view of their ionic radial and valences for maintaining the charge neutrality. In the present research, several compositions of Cu-Zn soft ferrites are synthesized, characterized and investigated. The ferrites under investigation are:

(i) $(Cu_{0.5}Zn_{0.5}Fe_{2-x})La_XO_4$ [x = 0.00, 0.05, 0.10]

(ii) $(Cu_{0.5}Zn_{0.5}Fe_{2-x})Sm_XO_4$ [x = 0.00, 0.05,0.10]

3.1.2 Method of Sample Preparation

Ferrites with optimized properties are always demanded delicate handling and caution approach in materials synthesis and appropriate knowledge of thermodynamics control of the chemical composition and homogeneity. As most of the properties

needed for ferrite applications are not intrinsic but extrinsic, preparations of ferrite samples has to encounter added complexity. There are many processing methods such as solid state reaction method [3.1], high energy ball milling [3.2], sol gel method [3.3], chemical co-precipitation method [3.4], microwave sintering method [3.5], auto combustion method [3.6] etc for the preparation of polycrystalline ferrite materials. They are mainly divided into two groups.

(i) Conventional Ceramic Method, i.e. Solid State reaction method, involves milling of reactants followed by sintering at elevated temperature.

(ii) Non-conventional method also called wet-method. Among these processes: Sol-Gel synthesis, chemical co-precipitation method, organic precursor method, reverse micelles method, co-spray roasting, activated sintering, etc.

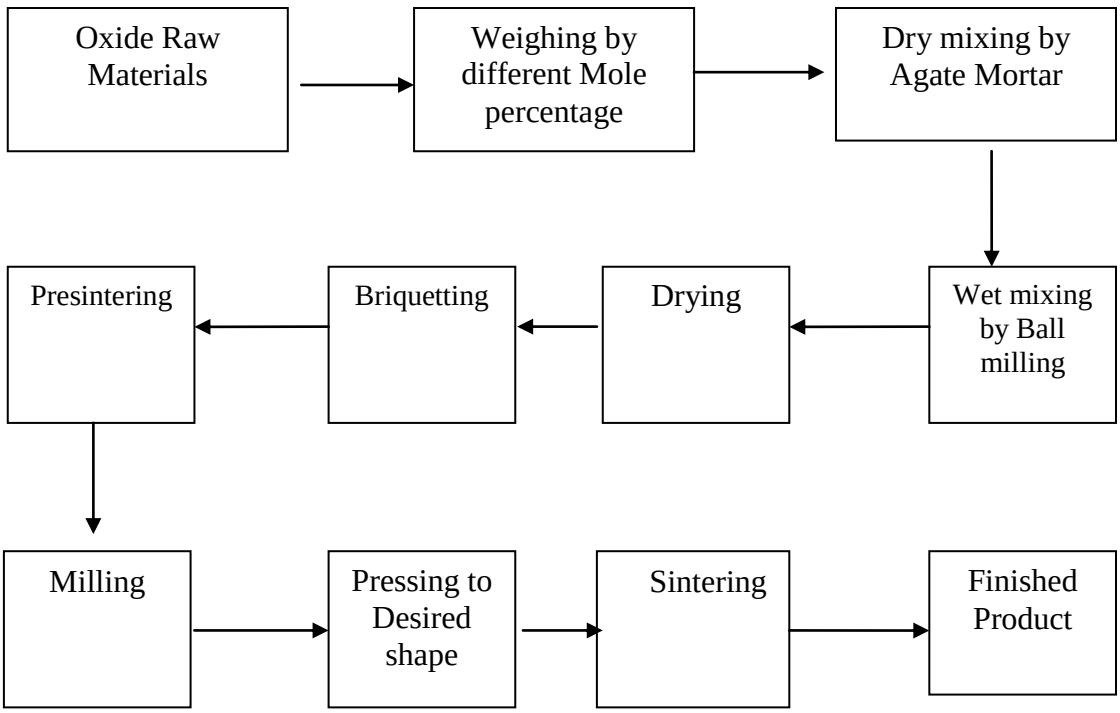

Figure 3.1: Flow chart of ferrite preparation.

The normal methods of preparation of ferrites comprise of the conventional ceramic method i.e. solid state reaction method involving hand milling of reactions following by sintering at elevated temperature range and non-conventional method, also called wet method chemical co-precipitation method and sol-gel method etc examples of wet method. The general preparation procedure of ferrites comprises of

the following operation as shown in figure 3.1. The block diagram and the detail of which are described subsequently.

3.1.3 Sample Preparation Technique

The ferrites of different compositions were prepared using ceramic technique involving solid state reaction from metal oxides (CuO, ZnO, La_2O_3, Sm_2O_3 and Fe_2O_3) in the form of grained powder having 99.99%. Different oxides were weighted precisely according to their molecular weight. The weight percentage of the oxide to be mixed for various samples was calculated by using formula. The appropriate weight percentage of each oxide to be mixed for different composition by the following formula:

Weight % of oxide

$$= \frac{Molecular\ \ weigh\ \ of\ \ oxide \times required\ \ weight\ \ of\ \ the\ sample}{Sum\ of\ \ molecular\ \ weight\ \ of\ \ each\ oxide\ in\ a\ sample}$$

The calculated weight of oxide materials, molecular weight of oxides and wt.% calculated for each sample prepared are used for experiments.

3.2 Solid State Reaction Method

This method was used the synthesis of Cu-Zn ferrites by many researchers [3.7-3.12]. In this method, different metal oxides are mixed and calcined to get ferrite powders. In the present investigation solid state reaction has been employed for the preparation of Cu-Zn ferrite samples for its simplicity and availability.

The overall preparation process generally comprised of the following four major steps:

(i) Preparing a mixture of desired composition

(ii) Pre-firing the mixture to form ferrite

(iii) Converting the “raw ferrite” into powder and pressing the powder into the required shapes

(iv)] Sintering

One thing is to be remembered that, the sintering process is irreversible in terms of microstructure, so that constant care could be maintained to keep conditions constant prior to and during sintering. A brief discussion given below will give us the idea about the above mentioned four major steps.

The sintering process is irreversible in terms of microstructure, so that constant care could be maintained to keep conditions constant prior to and during sintering. A brief discussion given below will give us the idea about the above mentioned four major steps.

3.2.1 Preparing a Mixture of Materials

The extend of this work in these step greatly, depending on the starting materials, when component oxide are used, the corresponding step involves a mere mixing of the oxides by wet milling. To avoid iron contamination, mixing is done with stainless steel balls in a steel ball milling machine and a fluid such as distilled water is used to prepare the mixture into slurry. Ferric oxide, Fe_2O_3 and whatever oxides, MO are required are taken in powder form with the captions in the ratio corresponding to that in the final product. Metal carbonate may also be used; during the later firing, CO_2 will be given off and they will be converted to oxides.

3.2.2 Pre-sintering the Mixture to Form Ferrite

The slurry prepared in step-1 is dried, palletized and then transferred to a porcelain crucible for pre sintering in a constant temperature of 1000°C for 4 hours. Presintering of the materials was preformed in a furnace named Gallen Kamp at AECD (Atomic Energy Centre, Dhaka). The cooling and heating rates were 4°C/min. The pre-sintering is very crucial because in this step of sample preparation of ferrite is formed form its component oxides. The solid-state reactions, leading to the formation of ferrites, actually achieved by counter diffusion. The ferrite is formed essentially in the pre-sintering step but the ‘raw’ ferrite formed has poor quality. In order to produce chemically homogeneous, dense and magnetically better material of desired shape and size, sintering at an elevated temperature is needed. The following block diagram in figure 3.4 represents the method employed for the Cu-Zn-rare earth ferrites.

3.2.3 Converting the Raw Ferrite into Powder and Pressing the Powder

Besides reducing the particle size to ≈1micron, grinding also eliminates intra particle pores and homogenizes the ferrite by mixing. To promote successful sintering in the next steps, the powder must be well characterized after grinding with respect to such factors as particles size and distribution, particle shape, homogeneity, absorbed gases, impurities and intra particle porosity. Iron contamination due to continuous wear of

the mill wall and steel ball need to be closely watched and minimized. Now to the ground homogeneous powder polyvinyl alcohol is added as a binder. Pressing the powder into compacts of desired shapes is done either by conventional method in a die-punch assembly or by hydrostatic or isocratic compaction. We made use of the former one. Pressing a uniformly dense body by this method is difficult owing to the friction gradient of the powder at the walls of the die and between the particles themselves. This problems is somewhat overcome by the addition of external and internal lubricant to the powder such as stearic acid. Mainly, we made two types of samples- tablet and toroidal. Specimen was prepared by a hydraulic press with a pressure of 2 ton/cm^2. The die was designed and made in the workshop of AECD. This is made of nonmagnetic stainless steel.

Figure 3.2: Hydraulic press used to make different shaped samples

These oxide mixtures were milled thoroughly for 4-6 hours to obtain homogeneous mixture. The mixture was dried and a small amount of saturated solution of polyvinyl alcohol (PVA) were added as a binder and pressed into pellet and toroid shape respectively under pressure 1.75 ton-cm^{-2} and 1.2 ton-cm^{-2} using hydraulic press figure 3.2. The prepared samples shown in figure 3.3 were sintered at

1100°C for 3 hrs with a microprocessor controlled muffle furnace. The samples were polished in order to remove any oxide layer formed during the process of sintering.

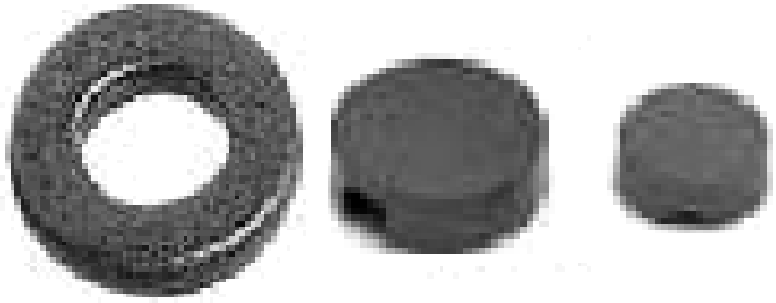

Figure 3.3: Toroid and disk shape sample

3.2.4 Sintering

Powder sintering involves raising the temperature of the green compact, (pressed powder part), to a certain level and keeping it at that temperature for a certain amount of time. The sintering temperature is usually between 70% and 90% of the melting point of the powder metal. This will cause bonding mechanisms to occur between powder particles pressed together in the compact. Bonding within the green compact is weak and this pressed unsintered part usually has just enough structural integrity to be handled. Bonding that occurs during sintering greatly strengthens the part.

Sintering involves heating the powdered metal compacts in vacuum or a reducing gaseous atmosphere to a temperature that is below the melting point of the primary constituent of the material. The metallic particles metallurgical bond and alloying take place via diffusion processes. Changes occur during sintering, including changes in size, configuration, and the nature of pores (figure 3.4). Commonly used atmospheres for sintering are hydrogen, carbon monoxide, and ammonia. Sintering operation ensures that powder particles are bonded strongly and that better alloying is achieved [1.13].

- This is a heat treatment by which a mass of compacted powder is transformed into a dense object. Sintering may result in densification, depending on the predominant diffusion pathway. It is used in the fabrication of metal and ceramic components, the agglomeration of ore fines for further metallurgical processing and occurs during the formation of sandstones and glaciers. Sintering must fulfill three requirements.

- To bond the particles together so as to impart sufficient strength to the product.
- To density the grain compacts by eliminating the pores and
- To complete the reactions left unfinished in the pre-sintering step.

The principle goal of sintering is the reduction of compact porosity. Sometimes the initial spaces between compacted grains of ceramics are called "voids", to differentiate term from the isolated spaces pores, which occur in the final stages of sintering. The sintering process is usually accompanied by other changes within the materials, some desirable and some undesirable

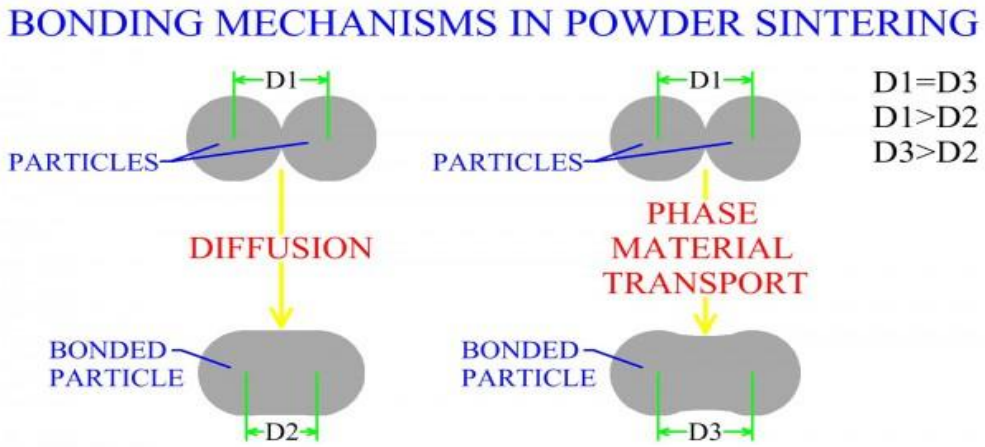

Figure 3.4: Bonding Mechanism in Powder Sintering.

The largest- changes occur in:

(i) Binding the particles together so as to impart sufficient strength to the products.

(ii) Densification the green compacts by eliminating the pores.

(iii) Making strength of elastic modulus

(iv) Making homogeneous distribution of grain number, grain size and shape.

(v) Developing the average pore size and shape.

. Sintering can be enhanced by the presence of a liquid phase.. The liquid phase can form directly from the elements when the sintering temperature is between the melting point of the matrix and the additive, by the melting of eutectic phase mixtures, which form by diffusion or by incipient melting. The liquid flows between the particles filling pores and causing densification by capillary action and through the provision of a fast diffusion pathway.

3.2.5 Necessity of sintering

The sintering process is usually accompanied by other changes within the materials, some desirable and some undesirable. The largest changes occur in;

i) To bind the particles together so as to impart sufficient strength to the products
ii) To make strength of elastic modulus
iii) To get a stable chemical composition and crystal structure
iv) To improve the average pore size and shape
v) To make homogeneous distribution of grain number, grain size and shape
vi) To make hardness and fracture tough
vii) To density the green compacts by eliminating the pores
viii) To homogenize the materials by completing the relation left unfinished in the pre-sintering step

The description of the sintering process has been derived from model experiments (e.g., sintering of a few spheres) and by observing powdered compact behavior at elevated temperatures. The following phenomena were observed:

(i) Increase of inter-particle contact area with time
(ii) Rounding-off of sharp angles and points of contact
(iii) In most cases, the approach of particle centers and overall densification
(iv) Decrease in volume of interconnected pores
(v) Continuing isolation of pores
(vi) Grain growth and decrease in volume of isolated pores

3.3 X-ray Diffraction (XRD)

X-rays are the electromagnetic waves whose wavelength is in the neighborhood of 1Å. X-ray diffraction (XRD) provides precise knowledge of the lattice parameter as well as the substantial information on the crystal structure of the material under study. The peaks in an X-ray diffraction pattern are directly related to the atomic distance. Let us consider an incident X-ray beam interacting with the atoms arranged in a periodic manner as shown in two dimensions in figure. 3.5. For a given set of lattice planes with an inter-plane distance of d, the condition for a diffraction (peak) to occur can be simple written as

$$2d \sin n\theta = n\lambda \ , \qquad (3.1)$$

which is known as Bragg's law. In the equation, λ is the wavelength of the X-ray, θ is the scattering angle, and n is an integer representing the order of the diffraction peak. The Bragg's Law is one of the most important laws used for interpreting X - ray diffraction data. From the law, we find that the diffraction is only possible when λ < 2d [3.14].

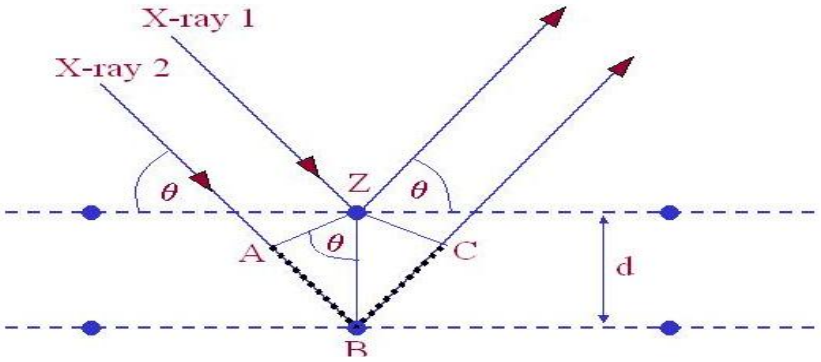

Figure 3.5: Bragg's diffraction pattern

In the present work, A PHILIPS PW 3040 X'pert PRO X-ray diffractometer was used for the lattice parameter to study the crystalline phases of the prepared samples in the Materials Science division, Atomic Energy Centre, Dhaka. figure 3.6 shows the block diagram of X' pert XRD system. The powder diffraction technique was used with a primary beam powder of 40 kV and 30mA for Cu-K_α radiation. A nickel filter was used to reduce Cu-K_β radiation and finally Cu-K_α radiation was only used as the primary beam. The experimental has been performed at room temperature. A 2θ scan was taken from 15° to 75° to get possible fundamental peaks of the samples with the sampling pitch of 0.02° and time for each step data collection was 1.0 sec.

All the data of the samples were stored in the computer memory and later on analyzed them using computer "software, X' PERT HJGHS CORE". For XRD experiment each sample was set on a glass slide and fixed the sample by putting adhesive typed the two ends of the sample. For each composition, the cylindrical samples of weight more than 2 gm are converted into powder. For XRD experiment each sample was set on a glass slide and fixed the sample by putting adhesive tape at the two ends of the sample X-ray diffraction patterns were carried out to confirm the crystal structure. Instrumental broadening of the system was determined from θ–2θ scan of standard Si. At (311) reflection's position of the peak, the value of instrumental broadening was found to be 0.07°. This value of instrumental broadening

was subtracted from the pattern. After that, using the X-ray data, the lattice constant (a) and hence the X-ray densities were calculated.

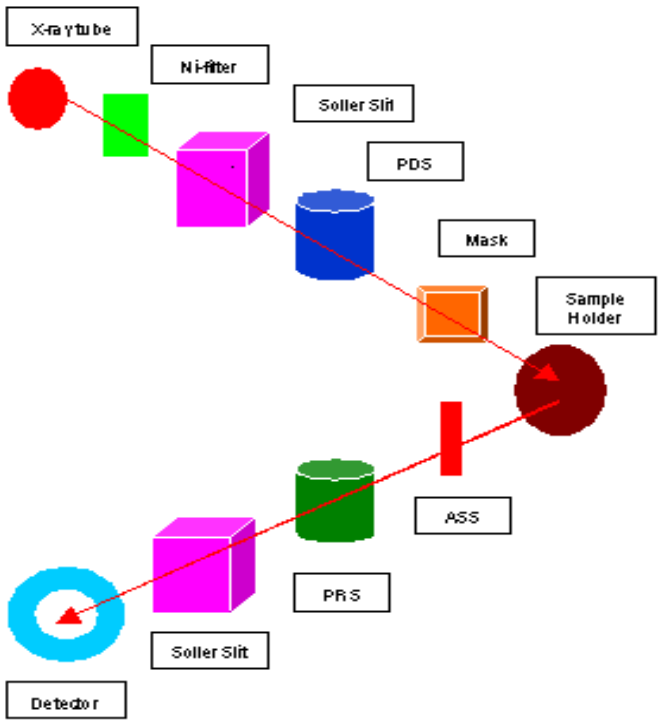

Figure 3.6: Block diagram of the PHILIPS PW 3040 X' Pert PRO XRD system

3.3.1 Different Parts of the PHILIPS X' Pert PRO XRD System

Figure 3.7 shows the inside view of the X' pert PRO XRD system. A complex of instruments of X- ray diffraction analysis has been established for both materials research and specimen characterization. These include facilities for studying single crystal defects, and a variety of other materials problems.

The PHILIPS X' Pert PRO XRD system comprised of the following parts;

(i) "Cu-Tube" with maximum input power of 60 kV and 55 mA,

(ii) "Ni- Filter" to remove Cu-K_α component,

(iii) "Solar slit" to pass parallel beam only,

(iv) "Programmable Divergent slits" (PDS) to reduce divergence of beam and control irradiated beam area,

(v) "Mask" to get desired beam area,

(vi) "Sample holder" for powder sample,

(vii) "Anti Scatter slit" (ASS) to reduce air scattering back ground,

(viii) "Programmable Receiving slit" (PRS) to control the diffracted beam intensity and

(ix) "Solar slit" to stop scattered beam and pass parallel diffracted beam only.

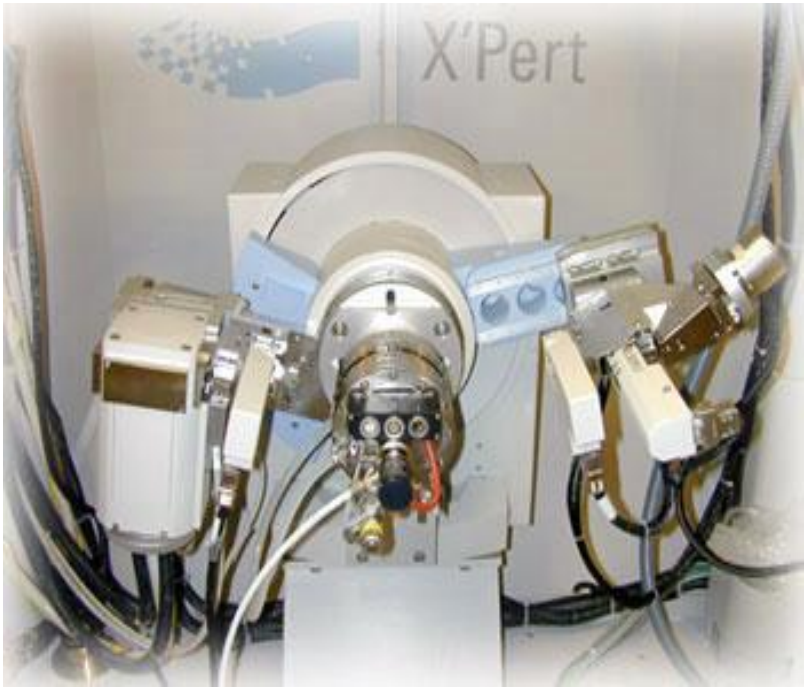

Figure 3.7: Internal arrangement of a PHILIPS X' Pert PRO X-ray diffractometer

3.3.2 Interpretation of the XRD data

The XRD data consisting of θ_{hkl} and d_{hkl} values corresponding to the different crystallographic planes are used to determine the structural information of the samples like lattice parameter and constituent phase. Lattice parameters of Cu-Zn ferrites samples were determined. Normally, lattice parameter of an alloy composition is determined by the Debye-Scherrer method after extrapolation of the curve. We determine the lattice spacing (interplaner distance), d using these reflections from the equation which is known as Bragg's Law.

$$2d_{hkl}\,\mathrm{Sin}\theta = \lambda$$

$$\text{i.e. } d_{hkl} = \frac{\lambda}{2\sin\theta}\ , \qquad (3.2)$$

where λ is the wavelength of the X-ray, θ is the diffraction angle and n is an integer representing the order of the diffraction.

The lattice parameter for each peak of each sample was calculated by using the formula:

$$a = d_{hkl} \times \sqrt{h^2 + k^2 + l^2} \quad , \tag{3.3}$$

where h, k, l are the indices of the crystal planes. We get d_{hkl} values from the computer using software "X' Pert HJGHS CORE". So we got ten 'a' values for ten reflection planes such as a a_1 , a_2 a_3 ….. etc. Determine the exact lattice parameter for each sample, through the Nelson-Riley extrapolation method. The values of the lattice parameter obtained from each reflected plane are plotted against Nelson-Riley function [3.15].The Nelson-Riley function F (θ), can be written as

$$F(\theta) = \frac{1}{2}\left[\frac{\cos^2\theta}{\sin\theta} + \frac{\cos^2\theta}{\theta}\right], \tag{3.4}$$

where θ is the Bragg's angle. Now drawing the graph of 'a' vs. F(θ) and using linear fitting of those points will give us the lattice parameter 'a_0'. This value of 'a_0' at F(θ) = 0 or θ = 90° .These 'a_0's are calculated with an error estimated to be ± 0.0001Å.

3.3.3 X-ray Density and Bulk Density

X-ray density, d_x was also calculated usual from the lattice constant. The relation between d_x and 'a' is as follows,

$$d_x = \frac{ZM}{Na^3}, \tag{3.5}$$

where M is the molecular weight of the corresponding composition, N is the Avogadro's number ($6.023X10^{23}$ $mole^{-1}$), 'a' is the lattice parameter and Z is the number of molecules per unit cell, (Z = 8 for the spinel cubic structure). The bulk density was calculated considering a cylindrical pellet of mass (m) and volume (V) of the pellets using the relation

$$d_B = \frac{m}{V} = \frac{m}{\pi r^2 h}, \tag{3.6}$$

where m is the mass of the pellet sample, r is the radius and h is the thickness of the pellet.

3.3.4 Porosity

Porosity is a parameter which is inevitable during the process of sintering of oxide materials. It is noteworthy that the physical and electromagnetic properties are strongly dependent on the porosity of the studied samples. Therefore an accurate idea of percentage of pores in a prepared sample is prerequisite for better understanding of the various properties of the studied samples to correlate the microstructure property relationship of the samples under study. The porosity of a material depends on the

shape, size of grains and on the degree of their storing and packing. The difference between the bulk density d_B and X-ray density d_x gave us the measure of porosity. Percentage of porosity has been calculated using the following relation [3.16]

$$P = (1 - \frac{d_B}{d_x}) \times 100\% \quad (3.7)$$

3.4 Permeability Measurement

3.4.1 Agilent Precision Impedance Analyzer (Wayne Kerr, 6500B)

Curie temperature measurements were done by using *Wayne Kerr, 6500B* impedance Analyzer shown in figure 3.8. Impedance parameters absolute value of impedance ($|Z|$), absolute value of admittance ($|Y|$), phase angle (θ), resistance (R), reactance (X), conductance (G), susceptance (B), inductance (L), capacitance (C), and quality factor (Q).

Moreover, the 4192A's high measurement performance and capable functionality delivers a powerful tool to circuit design and development as well as materials research and development (both electronic and non electronic materials) environments:

* Accurate measurement over wide impedance range and wide frequency range.
* Powerful impedance analysis function.
* Ese of use and versatile PC connectively.

The following are application examples;

- Impedance measurement of two terminal components such as capacitors, inductors, ferrite beads, resistors, transformers, crystal/ceramic resonators, multi-chip modules or array/network components.

Semiconductor components

- C – r characteristic analysis of varac for diodes.
- Parasitic analysis of a diode, transistor or IC package terminal/leads.
- Amplifier input/output impedance measurement.
- Impedance evaluation of printed circuit boards, relays, switches, cables, batteries etc.

Dielectric materials

- Permittivity and loss tangent evaluation of plastics, ceramics, printed circuit boards and other dielectric material

Magnetic materials

- Permeability and loss tangent evaluation of ferrite, amorphous and other magnetic materials.

Semiconductor material

- Permittivity, conductivity and C – V characteristics of semiconductor materials.

Figure 3.8: Impedance Analyzer Model-Wayne kerr,6500B

3.4.2 Permeability

From the frequency dependence of complex permeability, evolution of permeability and magnetic loss component at different stages of ferrite sample as affected by thermal treatment at different temperature was determined using toroids shape sample prepared with insulating Cu wire. The WK 6500B Impedance analyzer directly measure the value of inductance, L and loss factor.

$$D = \tan\delta \qquad (3.8)$$

From inductance the value of real part of complex permeability, μ' can be obtained by using the relation

$$\mu' = \frac{L}{L_0}\ , \qquad (3.9)$$

where L is the inductance of the toroid and L_o is the inductance of the coil of same geometric shape in vacuum, L_o is determined by using the relation,

$$L_0 = \frac{\mu_0 N^2 S}{\pi \bar{d}} \quad (3.10)$$

Here μ_o is the permeability of the vacuum, N is the number of turns (here N = 5), S is the cross-sectional area of the toroid shaped sample, S = dh, where, $d = \frac{d_1 \sim d_2}{2}$ and $\bar{d}$ is the average diameter of the toroid sample given as

$$\bar{d} = \frac{d_1 + d_2}{2}, \quad (3.11)$$

where, d_1 and d_2 are the inner and outer diameter of the toroid samples.

3.4.3 Mechanisms of Permeability

Mechanisms of permeability can be explained as the following way: a demagnetized magnetic material is divided into number of Weiss domains separated by block walls. In each domain all the magnetic moments are oriented in parallel and the magnetization has its saturation value M_s. In the walls the magnetization direction changes gradually from the direction of magnetization in one domain to that in the next. The equilibrium positions of the walls results from the interactions with the magnetization in neighboring domains and from the influence of pores; crystal boundaries and chemical in homogeneities which tend to favor certain wall positions.

3.4.4 Frequency Characteristic of Ferrite Samples

The frequency characteristics of the cubic ferrite sample i.e. the permeability spectra were investigated using a Impedance Analyzer of Model No.6500B provide the value of inductance, L and loss factor, D = tanδ. The measurements of inductances were taken in the frequency range of 1 kHz to 13 MHz. The values of measured parameters obtained as a function of frequency and the real (μ') and imaginary part (μ") of permeability and the loss factor are calculated. μ' is calculated by using the equation (3.9) and equation (3.10) and μ" is calculated by using the following equation $\mu'' = \mu' \tan\delta$ (3.12)

3.5 Materials Geometry

The AMH-series parameter measures characteristics of soft magnetic materials, according to the IEC 60404-4 and IEC 60404-6 standards. The ideal sample geometry of soft magnetic material is a ring. Thus shape is preferable because ring shape eliminates factors that can distort the magnetic test results. The main source of distortion of test data on soft magnetic materials is usually from air-gaps present in

the magnetic test circuit. These air gaps lower the apparent permeability of the material, and can be difficult to control. As ring geometry is continuous path, the magnetic circuit is closed, without any air gaps that cause distortion. If this machining process is on a sample must be form of ring can be made in different methods:

(i) made as an unique dense piece of material, obtained by mechanical works or by casting, sintering, etc.

(ii) made by stacking several disks with the same internal and external diameter, that can be obtained by punching, laser cutting, etc.

(iii) made by a unique thin strip wound as a clock-spring.

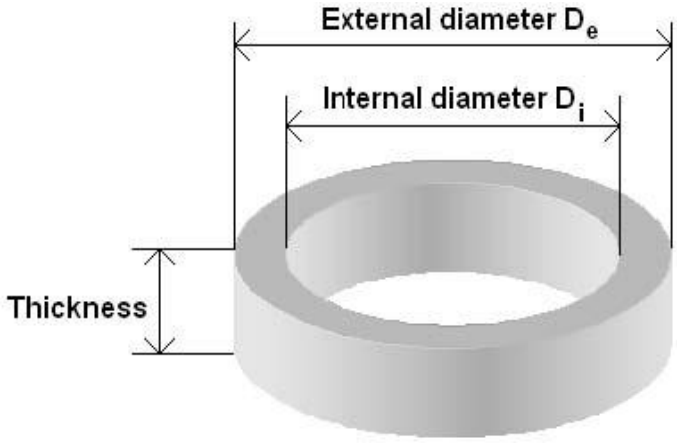

Figure 3.9: Sample geometry

The external diameter D_e should be higher than 1.4 times the internal diameter D_i. The cross section *A* of the sample is calculated by the geometrical relation

$$A = \frac{(D_e - D_i)h}{2}, \tag{3.13}$$

where *h* is the thickness of the sample. The thickness can be measured normally with a gauge if the sample is a solid ring. If it is made by stacked rings, sometimes it is preferred to use the mass and the density, calculating the thickness h with the formula:

$$h = \frac{4m}{\rho\pi(D_e^2 - D_i^2)}, \tag{3.14}$$

where ρ is the density of the material.

3.6 Dielectric Properties

Ceramics are mostly covalently bonded material hence electrically non conductive or insulator. Importance of particular property depends on the application demand. For instance, dielectric strength is an important parameter for application of ceramic as insulators used in power transmission line, load bearing general insulators,

in house hold appliances etc. In this kind of applications where frequency do not exceed 1kHz, the break down strength, measured in kV/cm, together with mechanical strength are important factors. The dielectric constant (ε') or loss factor (ε'') does not matter much. On the other hand, for capacitors and electronics application just the opposite required. The values of ε' and ε'' are of prime importance, not only their room temperature values but also as function of frequency. These are intrinsic properties of material, especially of polycrystalline ceramic can be modified by doping, micro structural variation.

3.6.1 Dielectric Constant

Dielectric constant measurements were done by using WK 6500B Impedance analyzer. The overall dielectric constant (ε') of an insulator material as given by the relation:

$$D = \varepsilon_0 E = \varepsilon_0 \varepsilon' E \tag{3.15}$$

D represents the electric displacement, E the electric field in the dielectric, ε' the dielectric constant and ε_0 permitivity of the vacuum. The electric displacement describes the extent to which the electric field has been altered by the presence of the dielectric material. The dielectric constant ε' is an intrinsic property of a material and a measure of the ability of the material to store electric charge relative to vacuum.

It is measured directly from the capacitance of a capacitor in which the material is used as electrode separator or dielectric. The capacitive cell, the dielectric constant (ε'), total charge (q) and capacitance © can be developed as follows:

$$\varepsilon' = \frac{D}{\varepsilon_0 E} = \frac{\frac{Q}{A}}{\frac{\varepsilon_0 V}{d}} \tag{3.16}$$

$$\therefore Q = \frac{\varepsilon_0 \varepsilon' A V}{d} = CV \tag{3.17}$$

Where $C = \frac{\varepsilon_0 \varepsilon' A}{d}$ (3.18)

Here A represents the area of the capacitive cell, d its thickness, C is the capacitance of the material, V the voltage across the cell and $\varepsilon_0\left(\frac{F}{m}\right)$ the material permittivity in vacuum.

Thus ε' represents the ratio of the permittivity or charge storage capacity relative to air or vacuum as dielectric

$$\varepsilon' = \frac{cd}{\varepsilon_o A}, \qquad (3.19)$$

where c is the capacitance of the pellet in Farad, d the thickens of the pellet in meter , A the cross-sectional area of the flat surface of the pellet in m^2 and ε_o the constant of permittivity for free space. Dielectric measurement as a function of frequency in the range 100Hz-13MHz at room temperature were carried out by using Hewlett Packrat impedance analyzer in conjunction with a laboratory made furnace which maintain the desired temperature with the help of a temperature controller.

3.7 Magnetization Measurement Techniques

Magnetization in ferrite samples originated due to the difference in the magnetic moments for the two sub-lattices. The larger the difference, the greater is the resultant magnetization, because of the anti-parallel arrangements of the moments in two sub-lattices. The magnetic moment of each sub-lattice arises due to the presence of magnetic ions such as Fe^{3+}, Fe^{2+}, Zn^{2+}, Cu^2 etc. in our case, only iron ion has magnetic moment since Mg non-magnetic. Different ions occupy different two sites. So, as a whole, the two sub-lattices have their individual resultant magnetic moments. The differences in magnetic moment between the two sub-lattices give rise to net magnetic moment which in turn yields magnetization. In the present study magnetization has been performed a Vibrating Sample Magnetometer (VSM).

3.7.1 Vibration Sample Magnetometer

The principle of vibrations sample magnetometer (VSM) is the measurement of electromotive force induces by magnetic sample when it is vibrate at a constant frequency in the presence of a static and uniform magnetic field. A small part of the (10 - 50 mg) was weighted and made to avoid movements inside the sample holder shown in Figure 3.10. VSM is a versatile and sensitive method of measuring magnetic properties developed by S. Foner [3.17] and is based on the flux change in a coil when the sample is vibrate near it. The simplest of these is the rotating coil which rotates at a fixed angular velocity. Therefore the amplitude of the generated voltage by rotating coil is proportional to the magnetic induction and therefore the amplitude can be used to measure magnetic induction or magnetic field in free space. The signal can be read directly as an AC voltage or converted to a DC voltage which is proportional to the amplitude. Figure 3.11 shows VSM of Model EV7 system.

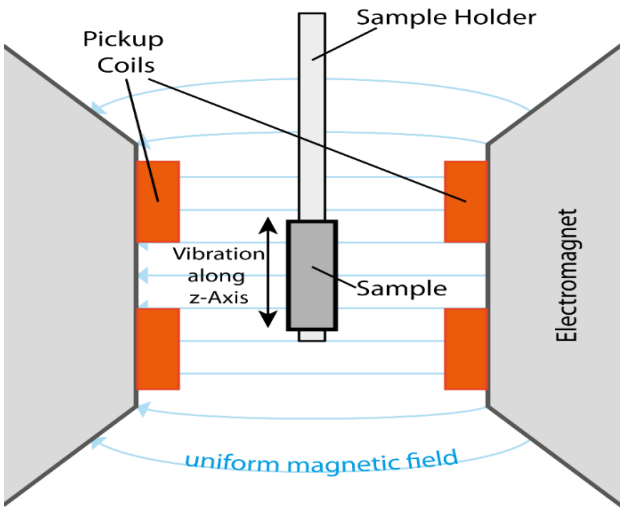

Figure 3.10: Vibrating Sample Magnetometer - sample holder and detection mechanism

The magnetic properties measurement system model EV7 is a sophisticated analytical instrument configured specially for the study of the magnetic properties of the small samples over a broad range of temperature from 103K to 800K and magnetic field from -20kOe to +20kOe. The VSM is designed to continuously measure the magnetic properties of materials as a function of temperature and the field. In this type of magnetometer, the sample is vibrated up and down in a region surrounded by several pick up coils. The magnetic sample is thus acting as a time-changing magnetic flux, varying the electric flux is accompanied by an electric field and the field induces a voltage in pick up coils. This alternating voltage signal is processed by a control unit system, in order to increase the signal to noise ratio. The result is a measure of the magnetization of the sample.

By using a compact gradiometer pickup coil configuration, relatively large oscillation amplitude (1- 3mm peak) and a frequency of 40 Hz, the system is able to resolve magnetization changes of less than 10^{-6} emu at a data rate of 1 Hz. The sample is attached to the end of a sample rod that is driven sinusoidal. The precise position and amplitude of oscillation is controlled from the VSM motor module using an optical linear encoder signal read back from the VSM linear motor transport. The voltage induced in the pickup coil is amplified and lock-in detected in the VSM detection module.

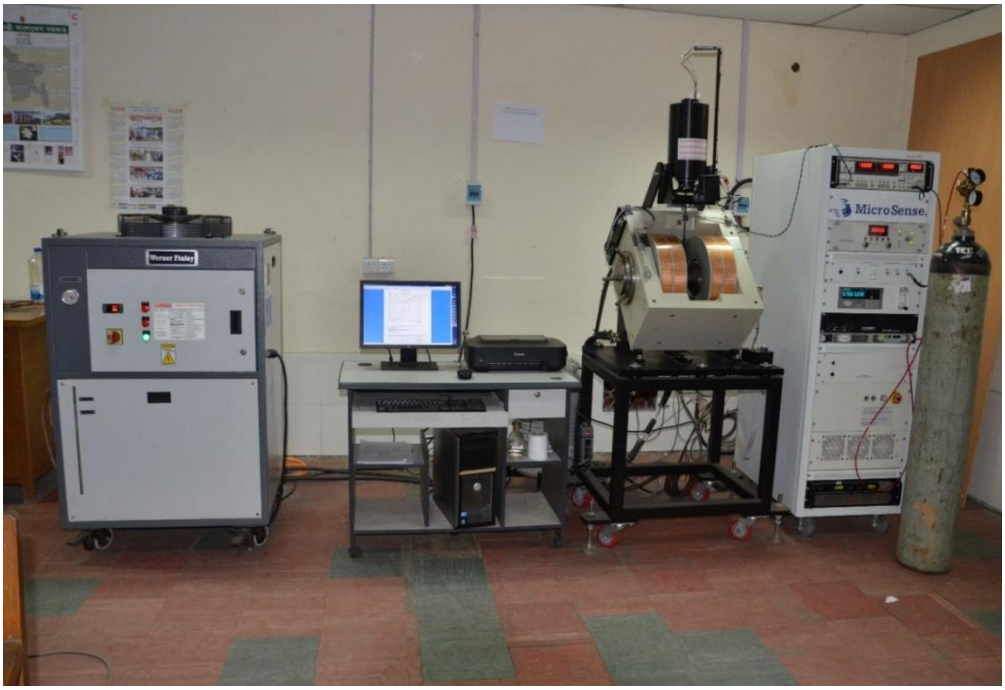

Figure 3.11: Vibrating Sample Magnetometer at Materials Science Division, AECD

The VSM detection module uses the position encoder signal as a reference for the synchronous detection. This encoder signal is obtained from the VSM motor module, which interprets the raw encoder signals from the VSM linear motor transport. The sample is fixed to sample holder located at the end of a sample red mounted in a electromechanical transducer. The transducer is driver by a power amplifier which itself is driver by an oscillator at a frequency of 90Hz. So, the sample vibrates along the 2-axis perpendicular to the magnetizing field. The latter induce a signal in the pick-up coil system that is fed to a differential. The output of the differential amplifier is subsequently fed into a tuned amplifier and an internal lock in amplifier that receives signal supplied by the oscillator. The output of the lock-in amplifier, or the output of the magnetometer itself, is a DC signal proportional to the magnetic moment of the sample being studied. Calibration of the VSM is done by measuring the signal of a pure Ni standard of Known saturation magnetic moment placed in the saddle point. The basic instrument included the electromechanical system and the electronic system including in personal computer. Laboratory electromagnet coils of various maximum field strengths may be used.

RESULTS AND DISCUSSION

4.0 Introduction

The rare earth oxides are recently becoming the promising and potential additives for the improvement of the properties of ferrites. Physical, electrical and magnetic properties arise from the ability of the ferrites to distribute the cations among the available A and B sites, and the relative strengths of exchange interactions. The properties can be changed by substitutions various kinds of divalent cations or relatively small amount of rear earth ions. Many workers reported on the influence of different additions and substitutions on structural, electrical and magnetic properties of ferrites [4.1 – 4.3]. These properties are very sensitive to preparation environment such as sintering temperature, time and type of additives. Present study areaddition of small amount of rare earth ions to Cu-Zn ferrite samples produces a change in their structural, magnetic and electrical properties depending upon the type and the amount of rare earth elements used.

Rare earth element has large magnetic moments, large magnetocrystalline anisotropy and very large magnetostriction at low temperature due to their localized nature of 4f electrons being totally screened by 5s and 5p orbital. But solubility of rare earth substitution in the spinel ferrite show phase segregation and diffusion of rare earth species to the grain boundaries are extra crystalline phases like orthoferrites [4.4 - 4.5]. Substitution of rear earth for Fe^{3+} in the octahedral site may show some interesting electromagnetic properties.

Structural characterization and identification of phases is a prior for the study of ferrites. The structural, magnetic and electrical properties of various polycrystalline of $(Cu_{0.5}Zn_{0.5}Fe_{2-x})RE_xO_4$ [RE = La, Sm] ferrites where x = 0.00, 0.05, 0.10 ferrites are studied. Samples are prepared with solid state reaction method and sintered at temperature 1100^0C for three hours. Optimum structural, electrical and magnetic properties of the ferrites necessitate have been investigated with variation Fe-deficient in Cu-Zn ferrites. The magneto transport properties are discussed for different concentration of La, Sm substitution on Cu-Zn ferrite. The effects of La^{3+} and Sm^{3+} substitution on the density, permeability, magnetic loss, saturation magnetization and dielectric constant of Cu-Zn-RE ferrites.

4.1 X-Ray Diffraction Analysis

X-ray neutron and electron diffraction are useful techniques to evaluate the various phases of the synthesized ferrites as well as their unit cell parameters. In the present study X-ray diffraction technique has been utilized to discern these parameters X-ray diffraction (XRD) studies of the samples were performed by using Philips PERT PRO X-ray Diffraction using Cu-K_α radiation in the range of $2\theta = 20^0$ to 70^0 in steps of 0.02^0.

4.1.1 Phase Analysis

The phase formation behavior of $Cu_{0.5}Zn_{0.5}Fe_2O_4$ ferrite sintered at 1100^0C for three hours are studied by XRD. All the samples show good crystallization with well defined diffraction lines. The XRD patterns for all the samples were indexed for fcc spinel structure and the Bragg planes are shown in the patterns. The XRD patterns of the samples are given in figure 4.1.

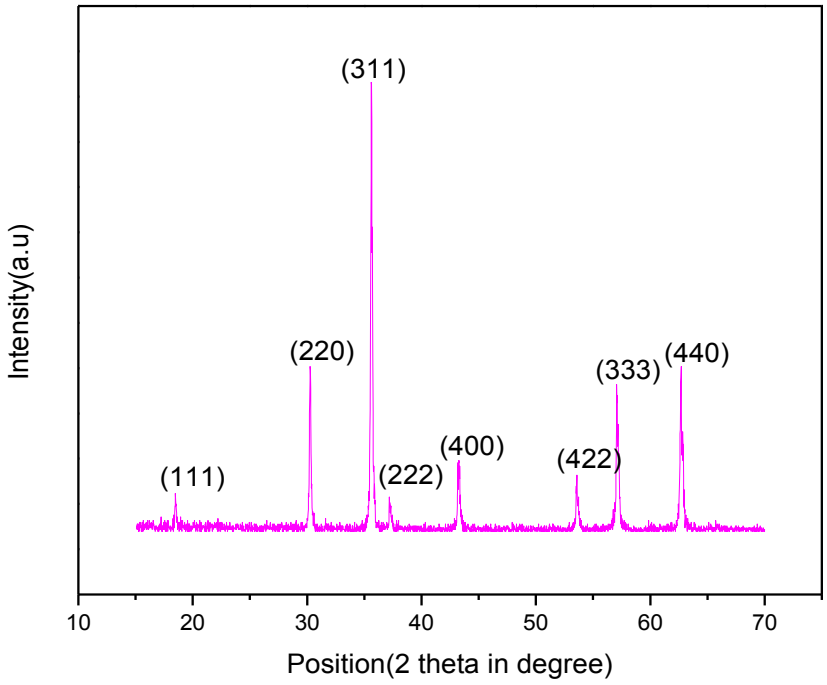

Figure 4.1: X-ray diffraction patterns of$Cu_{0.5}Zn_{0.5}Fe_2O_4$ ferrites sintered at 1100^0Cfor 3 hours

The peaks (111) (220), (311), (222), (400), (422), (333) and (440), which represents either all odd or even indicating that the samples are correspond to spinel phase which are characteristic of spinel structures with a single phase. The samples have been characterized as cubic spinel structure without any extra peaks corresponding to any second phase. Rare earth free sample show good crystallization with well defined diffraction line.

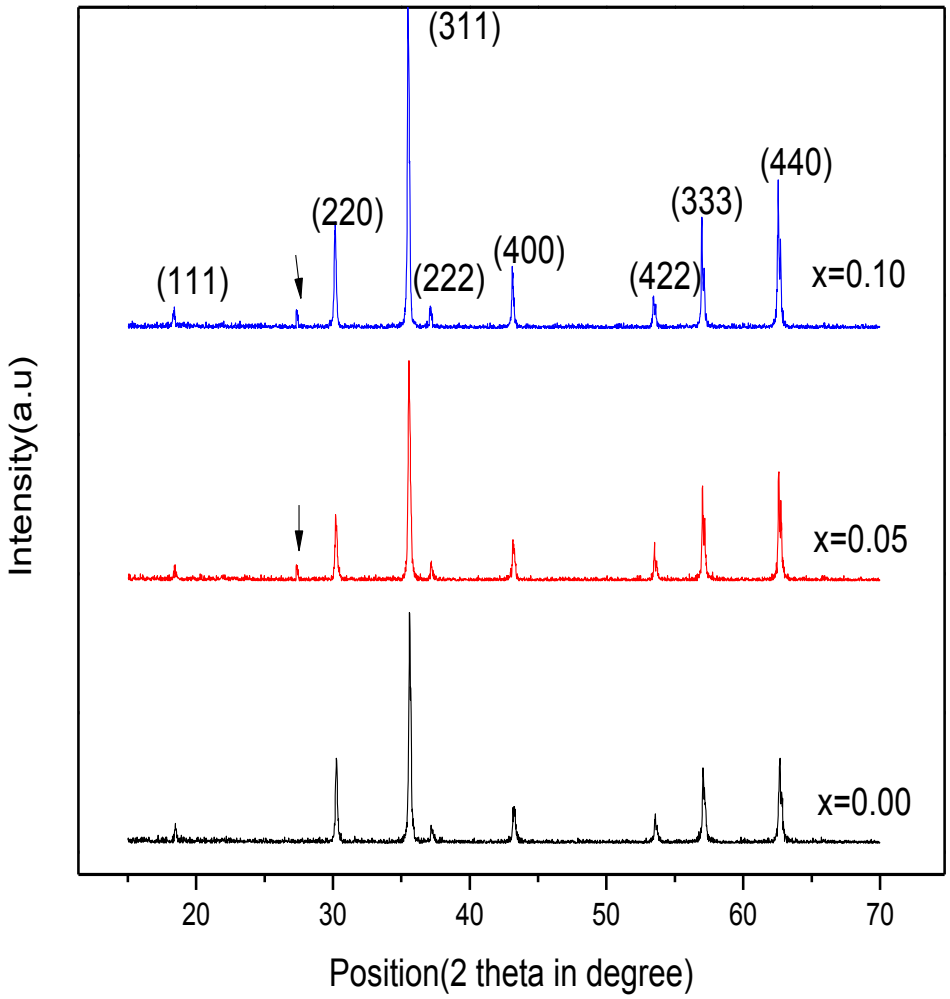

Figure: 4.2: X-ray diffraction patterns of $(Cu_{0.5}Zn_{0.5}Fe_{2-x})La_xO_4$[x= 0.05, 0.10] ferrites sintered at 1100Cfor 3 hours

The La substituted $(Cu_{0.5}Zn_{0.5}Fe_{2-x})La_xO_4$ferrites were extensively characterized by XRD shown in figure 4.2. The structural model was taken as the spinel phase was obtained for $(Cu_{0.5}Zn_{0.5}Fe_{2-x})La_xO_4$samples with x = 0.00, 0.05, 0.10.

However, a very weak reflection peak at $2\theta = 27.45^{\circ}$ is about to emerged for x = 0.05, 0.10 is more prominent indicated by the arrow. This peak was identified as the weak reflection peak of the $FeLaO_3$ phase.Table 4.1 shows the lattice parameters, bulk density, theoretical density and apparent porosity.

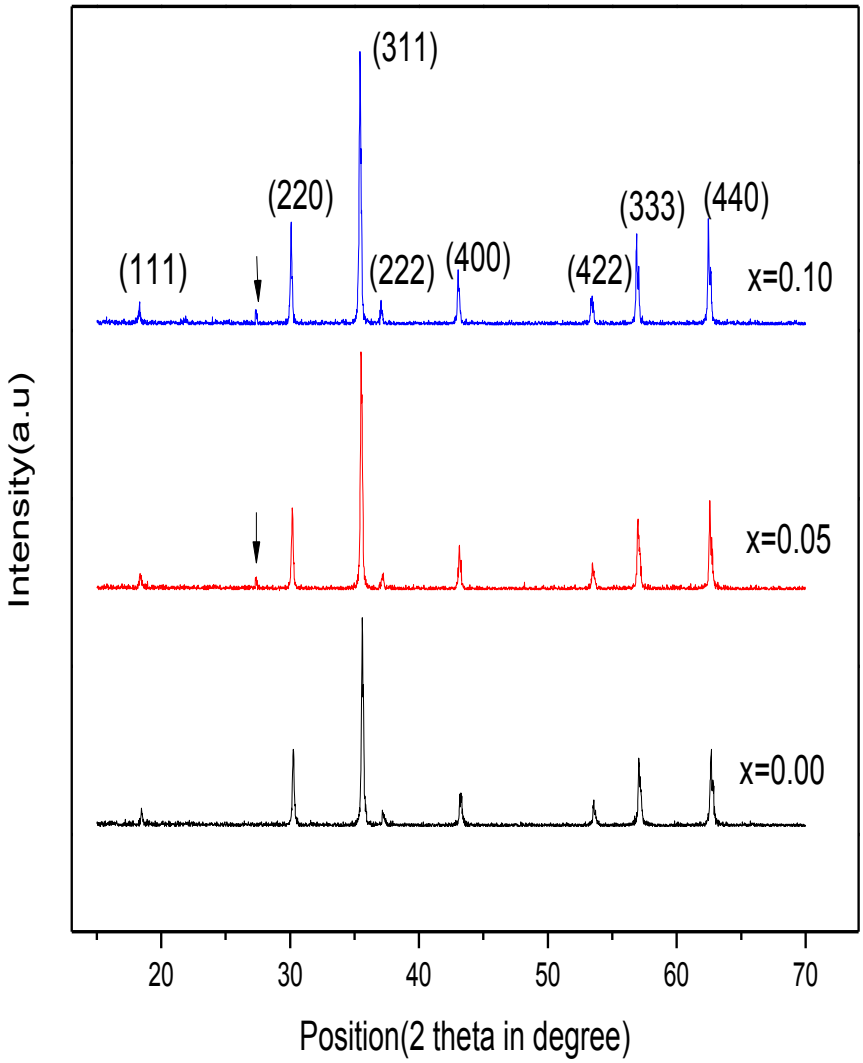

Figure 4.3: X-ray diffraction patterns of $(Cu_{0.5}Zn_{0.5}Fe_{2-x})Sm_xO_4$[x= 0.05, 0.10] ferrites sintered at 1100^0Cfor 3 hours

TheSm substituted $(Cu_{0.5}Zn_{0.5}Fe_{2-x})Sm_xO_4$ferrites where x =0.00, 0.05, 0.10 sintered at 1100^0C for 3 hours were studied by XRD. Figure 4.3 shows the XRD patterns of the as-burnt ferrite powders. The phase analysis revealed that the as burnt ferrite powders were crystalline in nature and the peaks (220), (311), (222), (400),

(422), (333) and (440) correspond to spinel phase which are characteristic of spinel structures with a single phase. The lattice parameter 'a' corresponding to each plane was calculated by using the X-ray data.

To identify the possible formation of a second phase $SmFeO_3$ formed in the substituted Sm in Cu-Zn ferrites, the amount of $SmFeO_3$, that is its peak intensity increased with increasing Sm concentration. This apparently indicated the Sm did not form a solid solution with spinel ferrites or it had very small solid solubility. Table 4.2 shows the lattice parameters, bulk density, theoretical density and apparent porosity.

4.1.2 Lattice Parameters

The values of the lattice parameters has been obtained from each plane are plotted against Nelson-Riley function [4.6] $F(\theta)=\frac{1}{2}\left[\frac{Cos^2\theta}{Sin\theta}+\frac{Cos^2\theta}{\theta}\right]$, where θ is the Bragg's angle by extrapolating lattice parameter's value of Fe(θ) = 0 or 90^o.

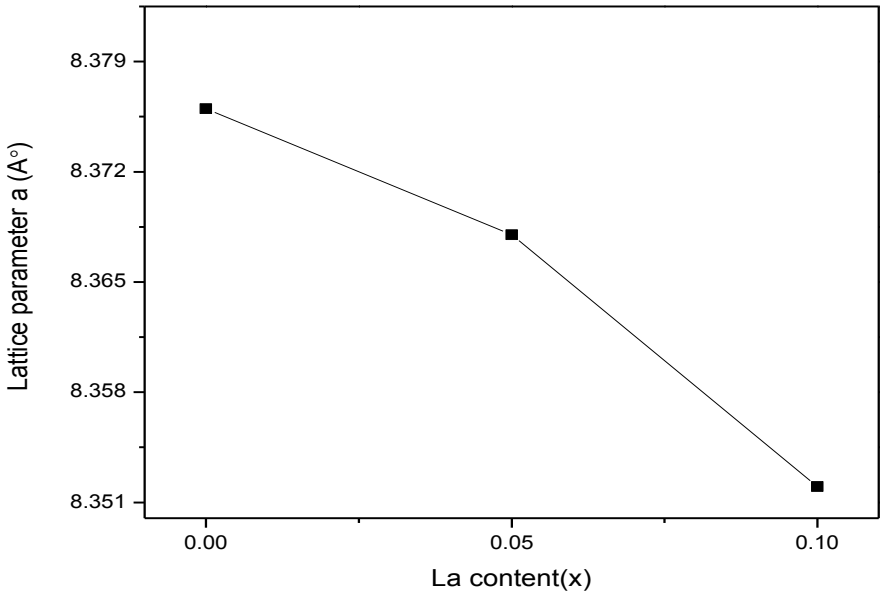

Figure 4.4: Lattice parameters calculated from X-ray diffraction patterns plotted as a function of La content in the series $(Cu_{0.5}Zn_{0.5}Fe_{2-x})La_xO_4$.

The variation of lattice parameter 'a' as a function of La^{3+} content x is shown in figure 4.4. A decrease in lattice constant is observed with the increasing of La content (x). This is indicates that the present system obeys the Vegard's law [4.7]. This may be due to La^{3+} ions having larger ionic radius ($1.03A^0$) [4.8] than that of

Zn^{+2} ions of ionic radius $0.68A^0$ [4.9]. The decrease in 'a_O' is probably due to a distribution in the spinel lattice because of the relatively large radius of La^{3+} shown in table 4.1. This is evidence by the appearance of the minor $LaFeO_3$ phase, besides the major spinel phase.

Table 4.2 shown in a minor decrease in 'a_0' of $(Cu_{0.5}Zn_{0.5}Fe_{2-x})Sm_xO_4$ ferrite with Sm substitution, which might be due to the compressive pressure exerted on the ferrite lattice by $SmFeO_3$. However, no significant decrease in 'a_0' is observed in the present experiment. There is a slight decrease Sm^{3+} (radius = 1.09Å) in the octahedral sites, indeed, lattice parameter was in the same range of different. This decrease can be attributed to the vacancy created by Zn^{2+} deficiencies with increasing its Sm^{3+} or La^{3+} content. The unit cell is expected to reduce is size by contraction of the lattice resulting in decrease of lattice parameter gradually

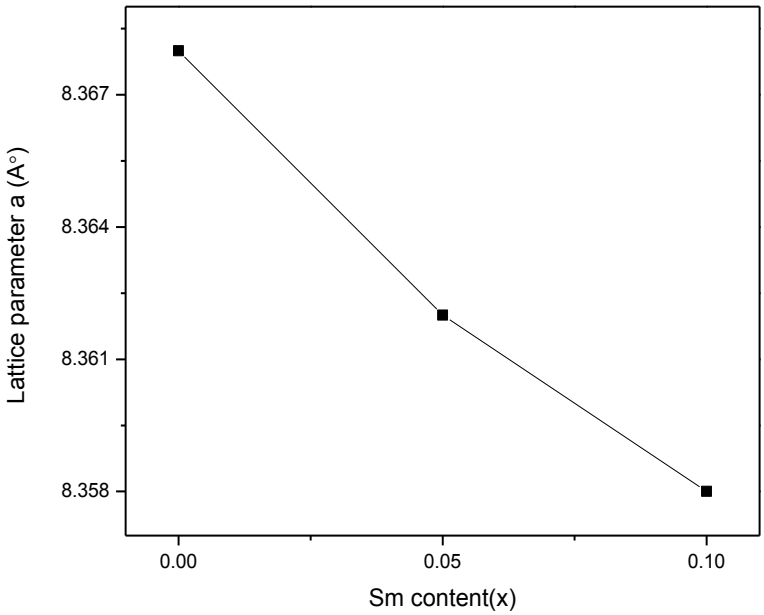

Figure 4.5: Lattice parameters calculated from X-ray diffraction patterns plotted as a function of Smcontent in the series $(Cu_{0.5}Zn_{0.5}Fe_{2-x})Sm_xO_4$

4.1.3 Density and Porosity

The bulk density (d_B) was measured by usual mass and dimensional consideration whereas X-ray density (d_x) was calculated from the molecular weight and the volume of the unit cell for each sample by using the equations(4.1) and (4.2).

$$d_B = \frac{m}{V} = \frac{m}{\pi r^2 h} \qquad (4.1)$$

$$d_x = \frac{8M}{Na^3} \, gm/cm^3 \qquad (4.2)$$

The calculated values of the bulk density and theoretical (or X-ray) density of the present ferrite system are listed in table- 4.1for La substituted and table-4.2 for Sm substituted in Cu-Zn ferrites.

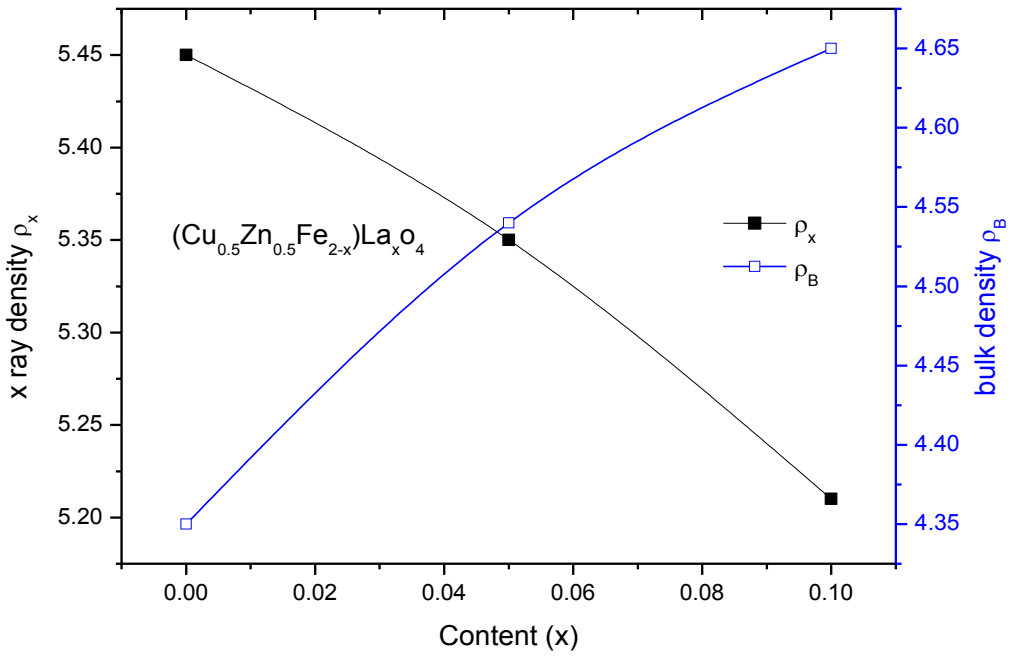

Figure 4.6: Variation of bulk density and X-ray density as a function of La content.

Figure 4.6 shows that X-ray density is higher than bulk density. This may be due to the porosity or voids into the samples are not considered in the X-ray density. In this case imaginary mass is considered instead of real mass. Bulk density increases with the increase of La content as shown in figure 4.6. Porosity also decreased with increasing of La content as shown in table 4.1. It was difficult to remove these closed porosity completely due to the evaporation of constituents especially Zn . Well known that the porosity of the samples come from two sources, intragranular porosity andintergranular porosity.Intergranular porosity mainly depends on the grain size

[4.10]. At higher sintering density temperatures the density is decreased because the intragranular porosity is increased resulting from discontinuous grain growth.

Table 4.1 Data of the lattice parameter (a), X-ray density (d_x), bulk density (d_B), porosity (P %) of $(Cu_{0.5}Zn_{.5}Fe_{2-x})La_x0_4$[x =0.00, 0.05 and 0.10]ferrites sintered at 1100^0Cfor 3 hours.

Sample composition	a_o ,(Å)	d_x(gm/cm^3)	d_B(gm/cm^3)	porosity%
$Cu_{0.5}Zn_{.5}Fe_2O_4$	8.376	5.45	4.35	20.18
$(Cu_{0.5}Zn_{.5}Fe_{1.95})La_{0.05}0_4$	8.368	5.35	4.54	15.14
$(Cu_{0.5}Zn_{.5}Fe_{1.9})La_{0.1}O_4$	8.352	5.21	4.65	10.74

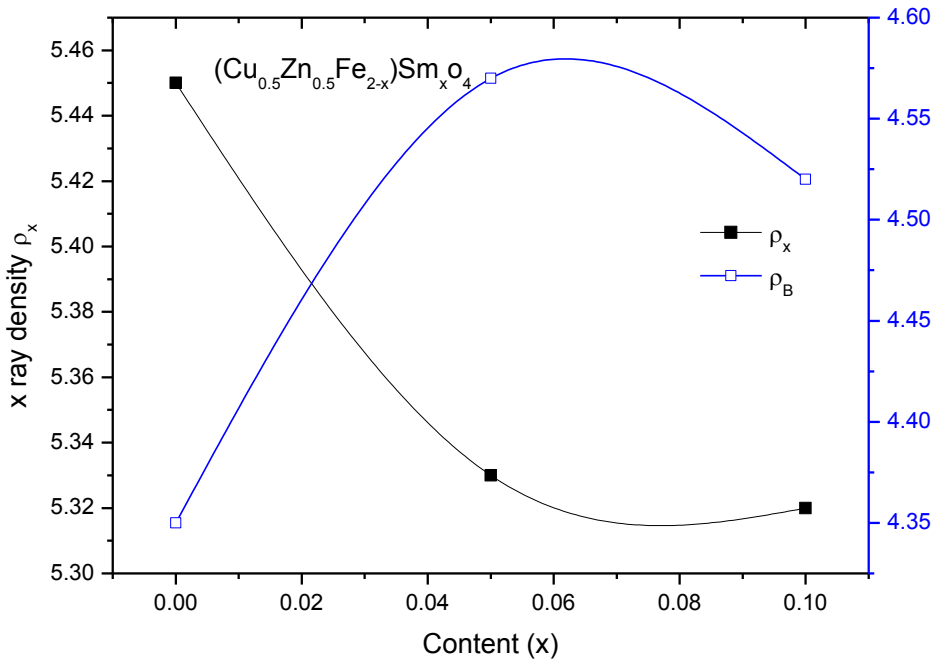

Figure 4.7: Variation of bulk density and X-ray density as a function of Sm content.

The X-ray density decreases continuously with increasing Sm content shown in figure 4.7. This may be due to the existence of pores which were formed and developed during the sample preparation or sintering process. The bulk density

initially increases with increasing rare earth ions Sm^{3+} finally minor decrease in with increase Sm substitution. It may be also be mentioned that reduction Fe^{2+} due to Fe^{3+} deficiency is expected to increase the resistivity of the samples.

This density plays an important role on the magnetic properties. Table-4.2 shows the results of lattice parameter, theoretical density, and bulk density calculated porosity for Sm doped Cu-Zn ferrites. The enhancement of Bulk density is due to activated diffusion process triggered by the excess vacancies created by Zn^{2+}deficiency. Specimens contained some closed porosity. It was difficult to remove these closed porosities completely due to the evaporation of constituents specially Zn. The intergranular porosity mainly depends on the grain size.

Table 4.2 Data of the lattice parameter (a), X-ray density (d_x), bulk density (d_B) of $(Cu_{0.5}Zn_{.5}Fe_{2-x})Sm_x0_4$[x =0.00, 0.05 and 0.10]ferrites sintered at 1100^0C for 3 hours.

Sample composition	$a_{o,}$(Å)	d_x(gm/cm^3)	d_B(gm/cm^3)	Porosity%
$Cu_{0.5}Zn_{.5}Fe_2O_4$	8.368	5.45	4.35	20.18
$(Cu_{0.5}Zn_{.5}Fe_{1.95})Sm_{0.05}0_4$	8.362	5.33	4.57	14.25
$(Cu_{0.5}Zn_{.5}Fe_{1.9})Sm_{0.1}O_4$	8.358	5.32	4.52	15.03

At higher sintering density temperatures the density is decreased because the intragranular porosity is increased resulting from discontinuous grain growth.

4.2 Frequency Dependence of Complex Permeability

The complex permeability is given by $\mu = \mu' - i\mu''$, μ' is the real permeability (in phase) and μ'' the imaginary permeability (90^0 out of phase). Complex permeability has been determined as a function of frequency up to 120MHz at room temperature for all the samples of series $(Cu_{0.5}Zn_{0.5}\ Fe_{2-x})\ La_xO_4$[x = 0.00, 0.05, 0.10] and $(Cu_{0.5}Zn_{0.5}\ Fe_{2-x})\ Sm_xO_4$[x = 0.00, 0.05, 0.10]ferrites by using the

conventional technique based on the determination of the complex impedance of circuit loaded with toroid shaped sample.

4.2.1 Frequency Dependence of Complex Initial Permeability La Substituted Cu-Zn Ferrites

Figure 4.8show the variation on real part of complex permeability μ' spectraas a function of frequency range 1kHz to 120MHz $(Cu_{0.5}Zn_{.5}Fe_{2-x})La_xO_4$for the different values of x at sintering temperature at 1100^0C for 3 hours. From these figure, it is seen that the real part of the permeability μ' remained almost constant until the frequency is raised to a certain value 10 to 30MHz and then drops to a very law values at higher frequencies for x = 0.05. It was interesting to note that the μ' significantly increases at x = 0.05 about $\mu' = 620$ and decreases at x = 0.10 of La substitution compared to that of un-doped sample about $\mu' = 215$. It is seen that the initial permeability at maximum about $\mu' = 620$ significantly increases at x = 0.05 of La substitution. La^{3+} has no unpaired electrons and it behaves as diamagnetic. The substitution of ferromagnetic Fe^{3+} by diamagnetic La^{3+} in the spinel is not useful for increasing permeability. It had been suggested substitution of La^{3+} ion moved Cu^{2+} and Zn^{2+} ion from 'B' to A' site causing 'A' sublattice dilution and increased the magnetic permeability in Cu-Zn ferrites.

In the present case La^{3+} incorporation into the lattice is very small (~ 0.05 atom/unit cell) and hence the increased permeability is do not due to its incorporation. The increased permeability at x = 0.05 compared to undoped one might be due to the following reason:

(i) Increased grain size, a specially increased crystallite size

(ii) Increased density as well as decreased porosity

(iii) Decreased magnetocrystalline anisotropy

(iv) Change in stress and

(v) Absence of the Cu-containing nonmagnetic precipitin compound due to the solid solution formation of Cu in $LaCuO_3$ phase etc.

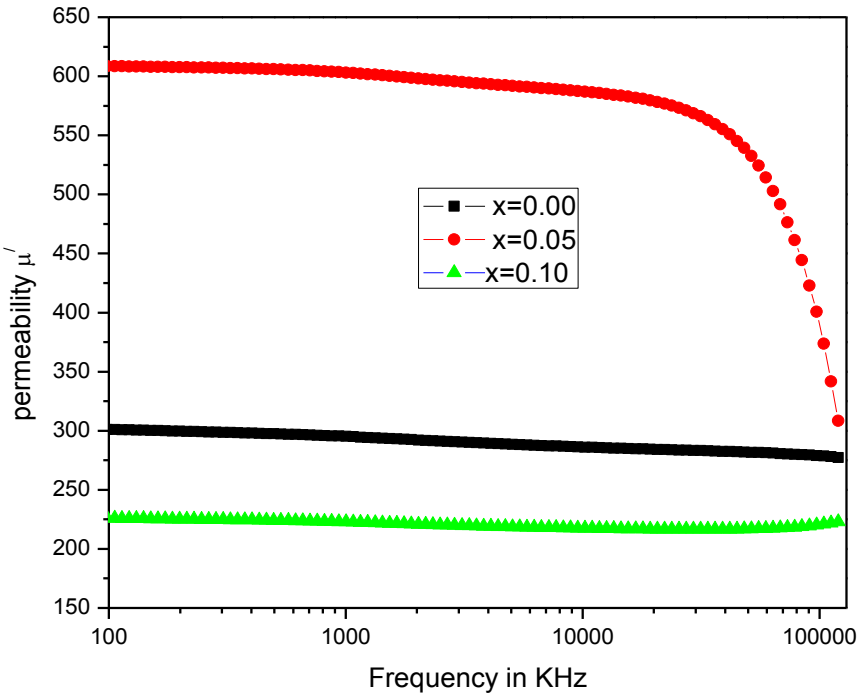

Figure 4.8: Variation of real part of initial permeability as a function of $(Cu_{0.5}Zn_{.5}Fe_{2-x})La_xO_4$ where x = 0.00, 0.05, 0.10 sintered at 1100^0C for 3 hours.

The La-substituted compositions were deficient in Fe and hence Fe^{2+} ions were expected to be at minimum. The magnetic anisotropy was also expected to decrease because magnetic anisotropy field in ferrites results mainly from Fe^{2+} ions [4.11]. This decrease in anisotropy increases the permeability. The decrease in initial permeability at x = 0.10 is probably due to minor precipitation of secondary phase $LaFeO_3$. That is, total initial permeability in this case is the sum of the contribution from the spinel and $LaFeO_3$ phase. The permeability of x = 0.05 composition is stable in the frequency range 1kHz to 30MHz. The dispersion of the other compositions were at higher frequency range stable compared to x = 0.05.The constant value of permeability over a wide frequency range, which is named the zone of utility of ferrites, is desirable over various applications such a broad band transformer and wide band read-writes head for video recording [4.12].

Figure 4.9 show the imaginary part of μ" gradually decreased with the frequency and attain state line at a certain frequency. At high frequencies where imaginary part of

permeability parameters become more significant, the inductors show high impedance and become resistive and dissipate interfering signals rather than reflecting these to the source.

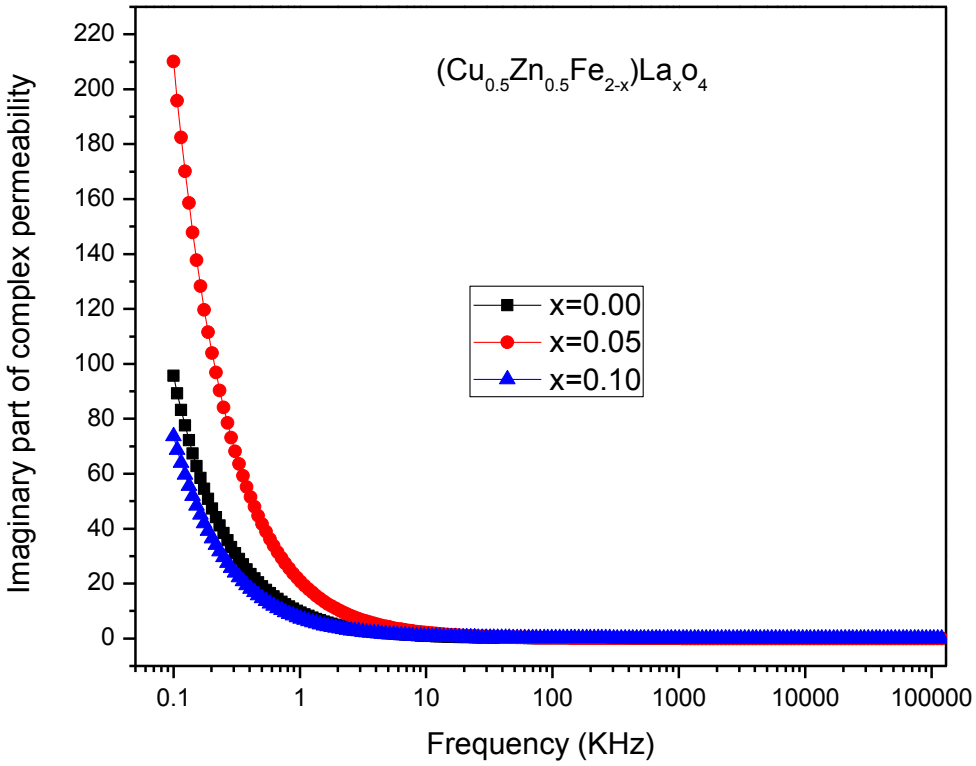

Figure 4.9: Variation of Complex imaginary permeability μ'' as a function of $(Cu_{0.5}Zn_{.5}Fe_{2-x})La_xO_4$ where x = 0.00, 0.05, 0.10 sintered at 1100^0C for 3 hours.

4.2.2 Frequency Dependence of Complex Initial PermeabilitySm Substituted Cu-Zn Ferrites

The optimization of the dynamic properties such as complex permeability in the high frequency range requires a precise knowledge of the magnetization mechanisms involved. From figure 4.10 it is noticed that the real component of permeability, μ' is fairly constant with frequency up to certain high frequency range, and then falls slowly value at maximum frequency. It is clearly evident from this figure that the initial permeability as a function of frequency in the range high MHz range and with decreases initial permeability with increase Sm content x monotonically. It is well established that permeability of polycrystalline ferrite

increases with increasing density and grain size. Decrease in permeability with Sm substitution might primarily be attributed to the increase in bulk density. An increase in the density, not only results in the reduction of demagnetizing field due to the reduction of pores but also raises the spin rotational contribution, which turns decrease the permeability.

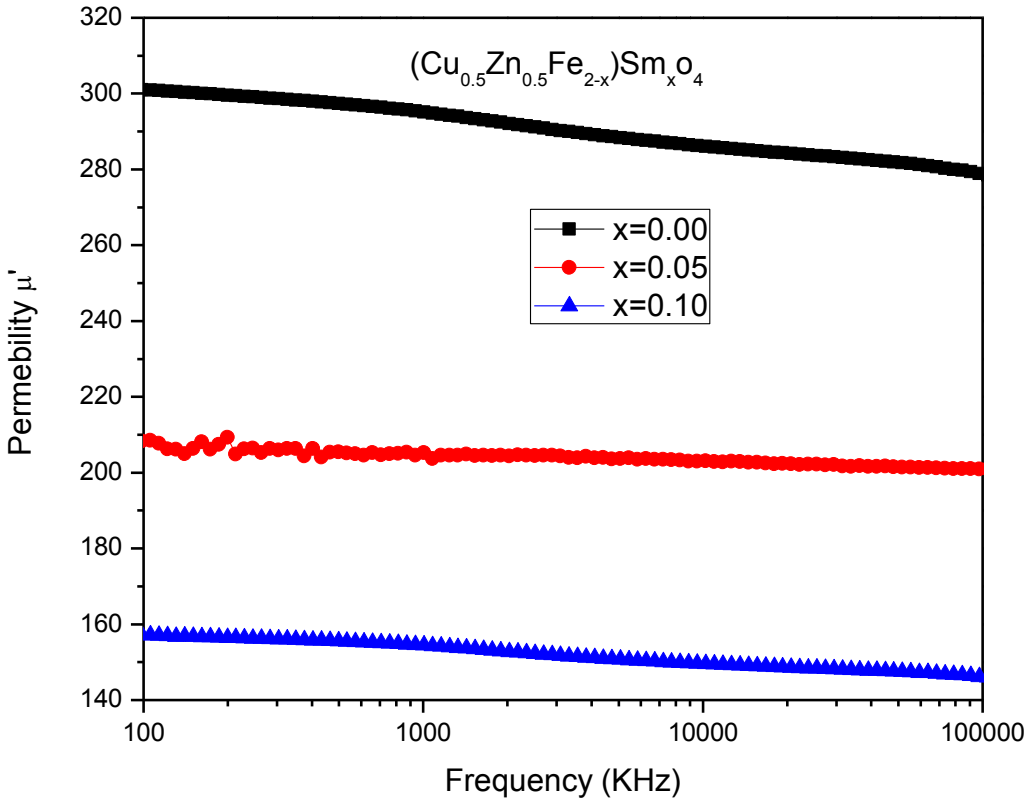

Figure 4.10: Variation of real part of initial permeability as a function of $(Cu_{0.5}Zn_{.5}Fe_{2-x})Sm_xO_4$ where x = 0.00, 0.05, 0.10 sintered at 1100^0C for 3 hours.

Figure 4.11 shows the imaginary part of complex permeability firs rises and suddenly decreases at low value at constant up to high frequency MHz range of are stable $(Cu_{0.5}Zn_{.5}Fe_{2-x})Sm_xO_4$ ferrites. When frequency is low, imaginary permeability is high and when frequency is high imaginary permeability is low. Thus an effective limit of product of frequency and imaginary permeability is established. So that effect of rare earth content of high frequency and high imaginary permeability are mutually incompatible.

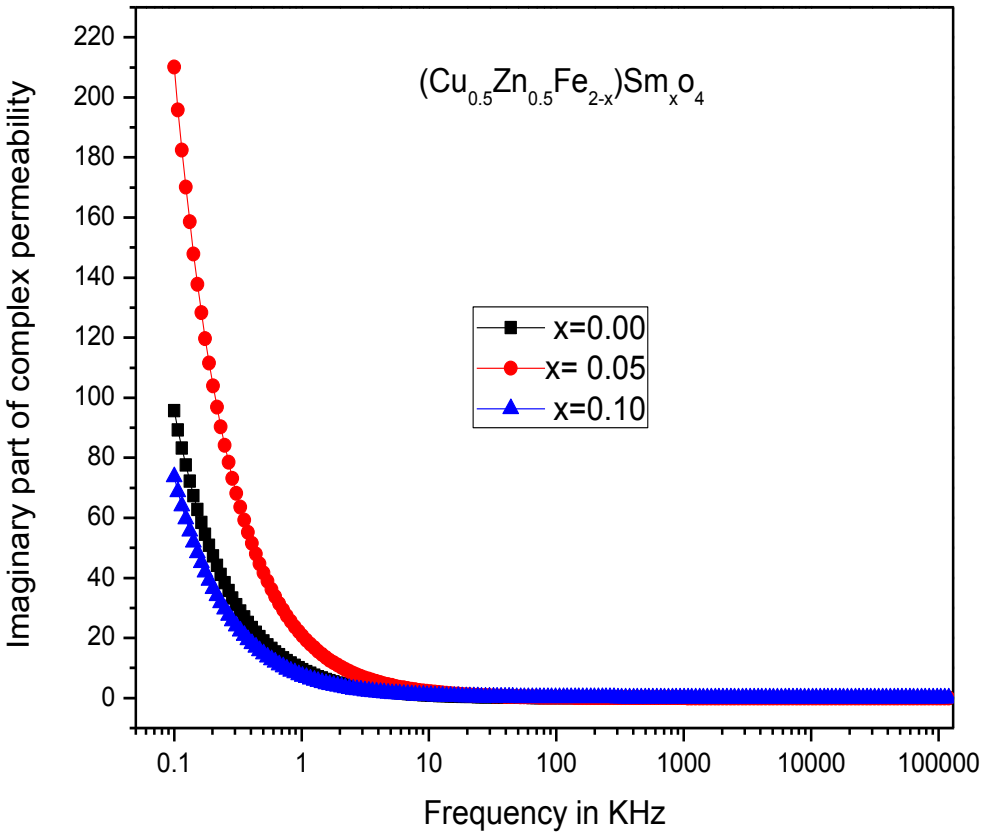

Figure 4.11: Variation of Complex imaginary permeability μ'' as a function of $(Cu_{0.5}Zn_{.5}Fe_{2-x})Sm_xO_4$ where x = 0.00, 0.05, 0.10 sintered at 1100^0C for 3 hours.

4.2.3Frequency Dependence of Quality Factor

The frequency dependence of $(Cu_{0.5}Zn_{0.5}\ Fe_{2-x})RE_xO_4$ (RE = La, Sm and x= 0.00, 0.05, 0.10) ferrites sintered at temperature at 1100^0C for 3 hours have been calculated from the relation Q = 1/ tanδ; where tanδ is the loss factor is used to measure the merit of the magnetic materials. Figure 4.12 and 4.13 shows the frequency dependence quality factors (Q-factors) of samples are $(Cu_{0.5}Zn_{.5}Fe_{2-x})La_x0_4$and $(Cu_{0.5}Zn_{.5}Fe_{2-x})Sm_x0_4$sintered at temperature at 1100^0C for 3hrs respectively. Q-factor increases with an increase of frequency showing a maximum value. The variation of the relative quality factor with frequency showed a similar trend for all the samples. Q-factor increases with increases of frequency showing no peak and peak must be may be > 120MHz range.

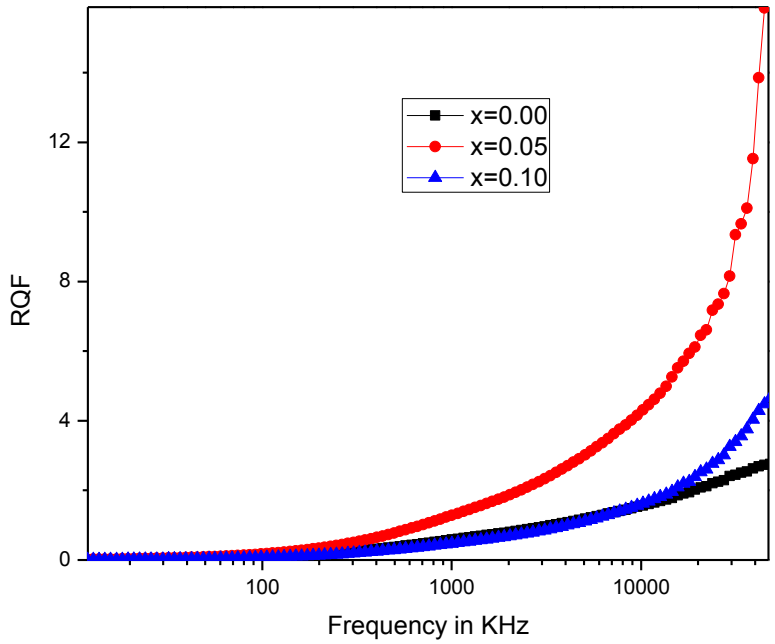

Figure 4.12: Variation of relative quality factor (RQF) as a function of $(Cu_{0.5}Zn_{.5}Fe_{2-x})La_xO_4$ where x = 0.00, 0.05, 0.10 sintered at 1100^0C for 3 hours.

The loss is due to lag of domain wall motion with respect to the applied alternating magnetic field and is attributed to various domain defects [4.13], which include non-uniform and non-repetitive domain wall motion, domain wall bowing, localized variation of flux density, nucleation and annihilation of domain walls. This phenomenon is associated with the ferromagnetic resonance within the domains [4.14] and at the resonance maximum energy is transferred from the applied magnetic field to the lattice resulting in the rapid decreases in RQF. Cu-Zn-La, Cu-Zn-Sm ferrites have been found to demonstrate reasonably good permeability at room temperature covering stable wide range of frequency indicating the possibilities for applications as high frequency up to several MHz induction and/or core materials. The corresponding to maxima Q-factor shifts to lower frequency range as increase of La or Sm content

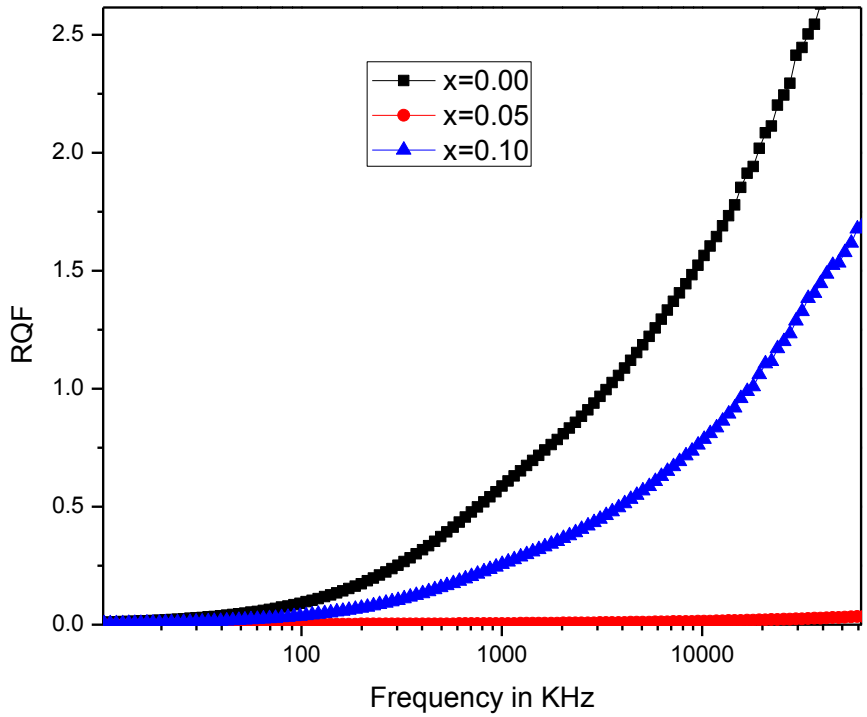

Figure 4.13: Variation of relative quality factor (RQF) as a function of $(Cu_{0.5}Zn_{.5}Fe_{2-x})Sm_xO_4$ where x = 0.00, 0.05, 0.10 sintered at 1100^0C for 3 hours.

4.3 Field Dependence of Magnetization of La Substituted Cu-Zn Ferrites

The Magnetization as a function applied field up to 12KOe measured with vibrating sample magnetometer (VSM) at room temperature of $(Cu_{0.5}Zn_{0.5}Fe_{2-x})La_xO_4$ ferrites sintered at 1100^0C for 3 hoursare shown in figure 4.14. It is observed that the magnetization increases sharply at very low field (H < 1KOe) which corresponds to magnetic domain reorientation that thereafter increases slowly up to saturation due to spin rotation. This magnetization process is connected with soft magnetic behavior of magnetic material. The slow process of magnetization toward the saturation value is connected with the magnetic anisotropy effect. Actual saturation could not be attained even with magnetic field as high as 12KOe.

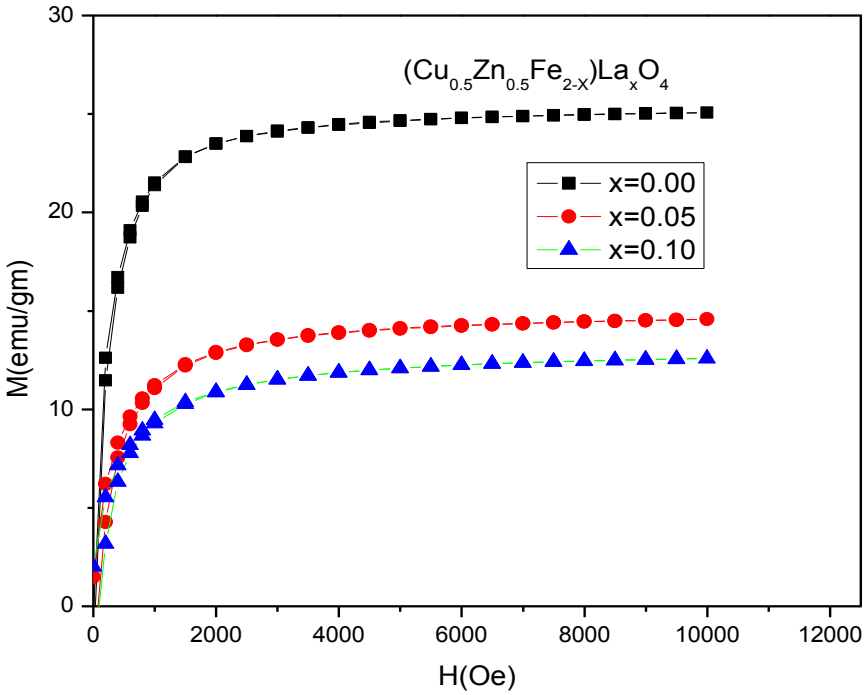

Figure 4.14: Variation of magnetization at room temperature as a function of applied field on $(Cu_{0.5}Zn_{.5}Fe_{2-x})La_xO_4$where x = 0.00, 0.05, 0.10 sintered at 1100^0C for 3 hours.

Figure 4.14 shows the variation of saturation magnetization (M_S) of decreases with increasing La content. The observed M_S can be explained on the basis of cation distribution and the exchange interaction A and B sites, respectively. In perfect ferrites, the A-A, B-B and A-B nearest neighbor exchange couplings are normally antiferromagnetic and the A-B exchange coupling is usually heavily predominant. The net magnetization is therefore the difference between the magnetic moments of B and A sublattices, i.e., $M = M_B - M_A$ and will normally be parallel to the B-sublattice magnetization because the number of cations on B-sites is twice the number of cations on A-sites. The magnetization of each composition on the distribution of Fe^{3+} ions between the two sublattices A and B, where the Zn^{2+} and Cu^{2+} and La^{3+} ions are nonmagnetic.

It is mentioned that $CuFe_2O_4$ and $ZnFe_2O_4$ ferrite are known as inverse ferrite, where Cu^{2+} ions are located on both sites, and Zn^{2+} ions are located on B-sites. The substitution will lead to decrease Fe^{3+} ions on the B-sites and consequently the

magnetization of the B-sites will decrease. At the same time the magnetization of A-sites will increase according to the increase of the Fe^{3+} ions on A-sites. So the net magnetization has decreases accordingly increasing La-content substituted Cu-Zn ferrites.

Table 4.3: Saturation magnetization (M_s) of $(Cu_{0.5}Zn_{0.5}Fe_{2-x})RE_xO_4$ [RE = La, Sm] where X= 0.00, 0.05, 0.10 ferrites

Name of samples	M_s	Name of samples	M_s
$Cu_{0.5}Zn_{0.5}Fe_2O_4$	25	$Cu_{0.5}Zn_{0.5}Fe_2O_4$	25
$Cu_{0.5}Zn_{0.5}Fe_{1.95}La_{0.05}O_4$	14	$Cu_{0.5}Zn_{0.5}Fe_{1.95}Sm_{0.05}O_4$	9
$Cu_{0.5}Zn_{0.5}Fe_{1.9}La_{0.1}O_4$	12	$Cu_{0.5}Zn_{0.5}Fe_{1.9}Sm_{0.1}O_4$	7

4.3.1 Field Dependence of Magnetization of Sm Substituted Cu-Zn Ferrites

Figure 4.15 shows the variation of magnetization of the $(Cu_{0.5}Zn_{0.5}Fe_{2-x})La_xO_4$ ferrites sintered at 1100^0C for 3 hours as a function of applied magnetic field for various where x = 0.00, 0.05 and 0.10 measured by VSM. It is observed that the magnetization increases sharply at very low field which corresponds to magnetic domain reorientation that thereafter increases slowly up to saturation due to spin rotation. This magnetization process is connected with soft magnetic behavior of magnetic material.

Figure 4.15 show the M_S values or saturate level of Smsubstituted ferrites is lower that unsubstituted specimen, might be due to better bulk density and decreases permeability with increasing Sm substituted. This has due to the presence of higher quantity of nonmagnetic $SmFeO_3$ phase. The decrease M_S seems that strong short range ferromagnetic ordering and frustration coexists with in the antiferromagnetic matrix. The observed decrease magnetization curves are mentioned of each composition on the distribution of Fe^{3+} ions between the two sublattices A and B, where the Zn^{2+} and Cu^{2+} and Sm^{3+} ions are nonmagnetic. Hence the present system

Sm substituted Cu-Zn ferrites, frustration and randomness decreases in M_S shows significant departure from Nell's collinear model.

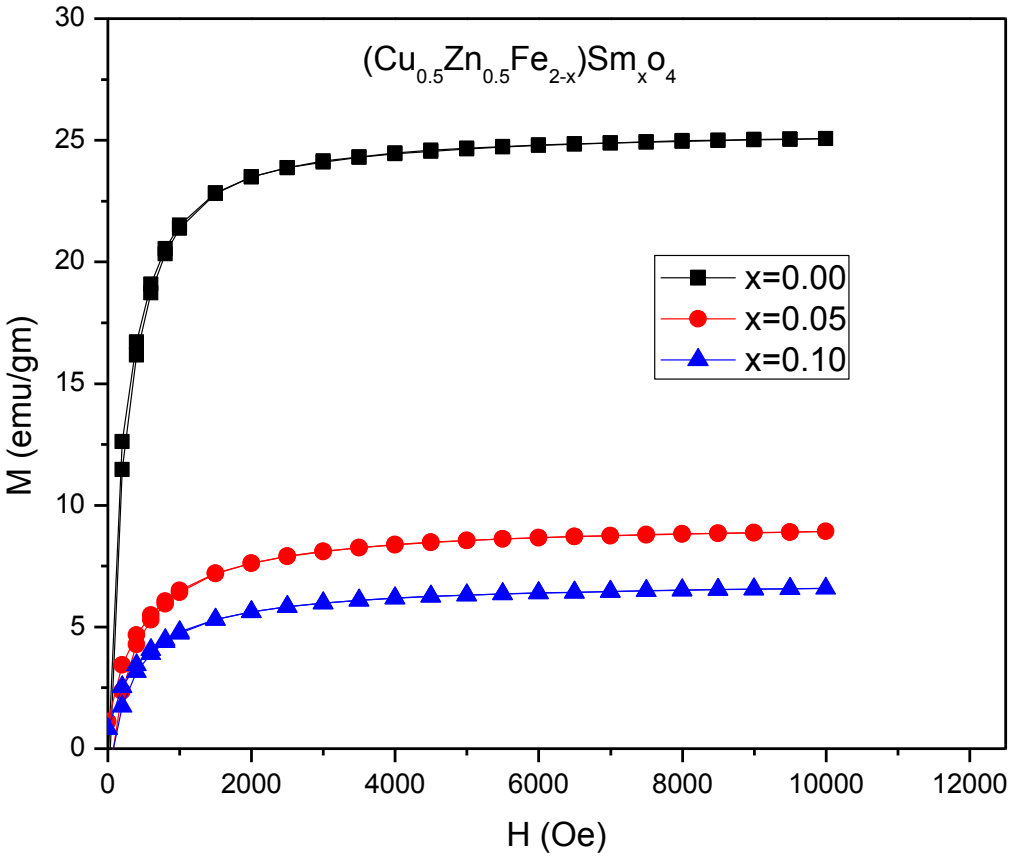

Figure 4.15: Variation of magnetization at room temperature as a function of applied field on $(Cu_{0.5}Zn_{.5}Fe_{2-x})Sm_xO_4$where x = 0.00, 0.05, 0.10 sintered at 1100^0C for 3 hours.

4.4 Frequency Dependence of Dielectric Constant

Figure 4.16 and figure 4.17 show the variation of dielectric constant, ε' with frequency for different composition of $(Cu_{0.5}Zn_{.5}Fe_{2-x})La_x0_4$ and $(Cu_{0.5}Zn_{.5}Fe_{2-x})Sm_x0_4$ where x = 0.00, 0.05, 0.10 ferrites sintered at 1100^0C for 3 hours 1MHz to 120MHz at room temperature. It can be seen from the figure that the dielectric constant is found to decrease continuously with increasing frequency for all the specimens exhibiting a normal dielectric behavior of ferrites. The dielectric dispersion is rapid at lower frequency region and it remains almost independent at high frequency side. The incorporation of rare earth elements La in figure 4.16 and Sm in figure 4.17 into these ferrites has no pronounced effect on the dielectric constant in high frequency, but significantly decreases the dielectric constant in the low frequency range.

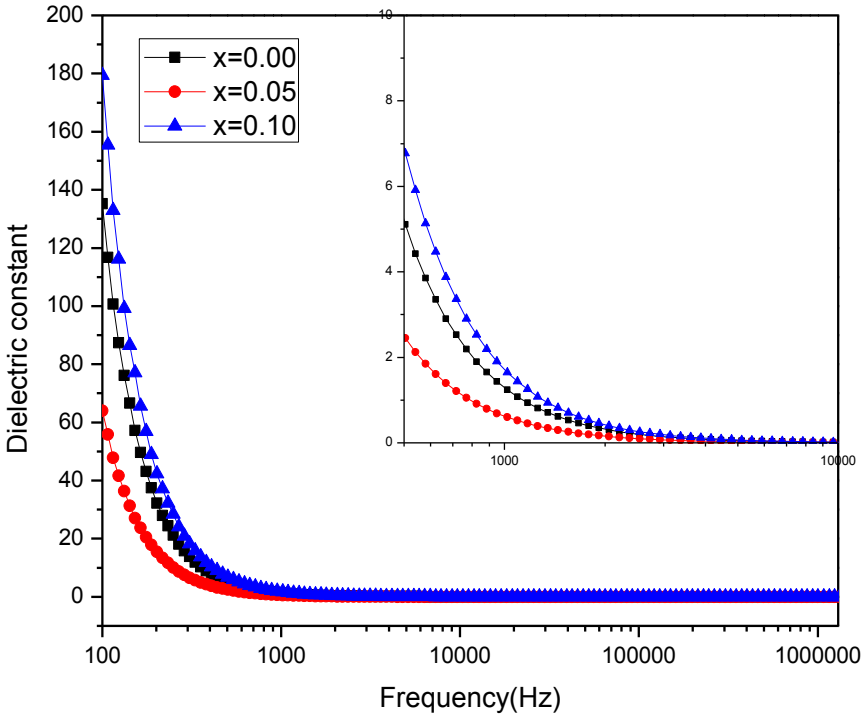

Figure 4.16: Variation Dielectric constant at room temperature as a function of frequency of the ferrite system on $(Cu_{0.5}Zn_{.5}Fe_{2-x})La_xO_4$where x = 0.00, 0.05, 0.10 sintered at 1100^0C for 3 hours.

The type of behavior was observed in a number of ferrites such as Li- Co ferrites [4.15], Cu – Cd ferrites [4.16], Ni–Cu–Zn ferrites [4.17], Mg–Cu–Zn ferrites [4.18- 4.19]. The dielectric behavior of ferrites may be explained on the basis of the mechanism of the dielectric polarization process and is similar to that of the conduction process. The electronic $Fe^{2+} \leftrightarrow Fe^{3+}$gives the local displacement of electrons in the direction of applied electric field, which induces the polarization in ferrites [4.20]. The La substituted Cu-Zn ferrites have high values of in the order of 6 to 18×10^{12} at low frequencies whereas Sm doped samples 6 to 13×10^{12} at low frequencies.

The magnitude of exchange depends on the concentration Fe^{2+}/Fe^{3+} in pairs present on B-site for the present ferrite. This could be explained using Koop's phonological theory [4.21], which has based on the Maxwell-Wagner model [4.22 - 4.23] for inhomogeneous double layer dielectric structure. The dielectric structure has supposed to be composed of the fairly well conducting ferrite grains.The first layer is the fairly well conducting large ferrite grain which is separated by the second thin

layer of the poorly conducting grain boundaries. The grain boundaries of the lower conductivity were found to be ferrite at lower frequencies while ferrite grains of high conductivity are effective at high frequency.

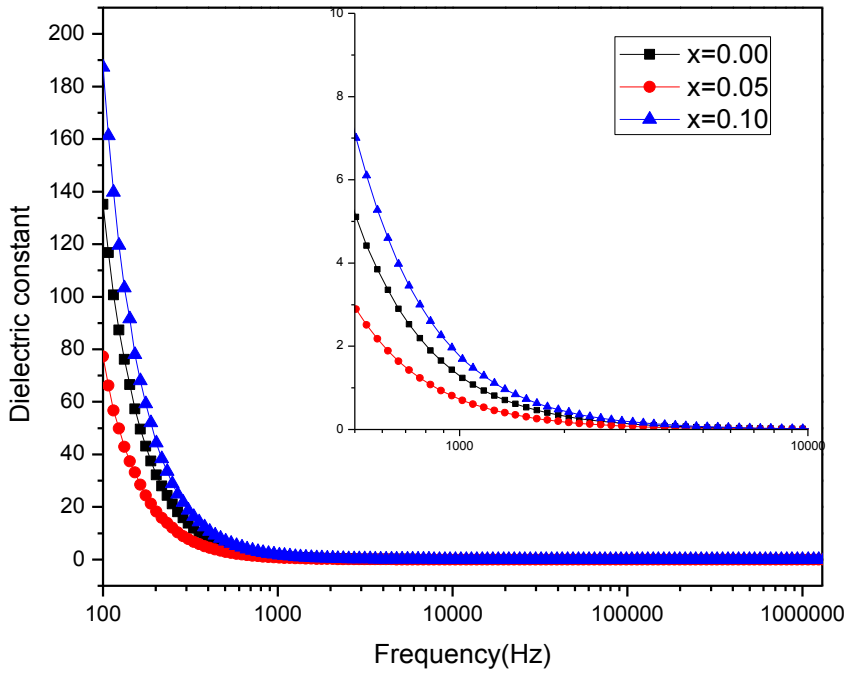

Figure 4.17: Variation Dielectric constant at room temperature as a function of frequency of the ferrite system on $(Cu_{0.5}Zn_{.5}Fe_{2-x})Sm_xO_4$ where x = 0.00, 0.05, 0.10 sintered at 1100^0C for 3 hours.

CONCLUSIONS

5.1 Conclusions

The present work has been focused on the effect of rare earth ions on the structural, magnetic and transport properties of $(Cu_{0.5}Zn_{0.5}Fe_{2-x})RE_xO_4$ ferrites where RE = La and Sm, [x = 0.00, 0.05 and 0.1] are prepared with solid state reaction method and sintered at 1100^oC for holding time 3 hours. The effects of La^{3+} and Sm^{3+} substitution on the density, permeability, magnetic loss, saturation magnetization and dielectric constant of Cu-Zn ferrites were also investigated. The XRD pattern confirmed the Cu-Zn ferrite sample is single phase spinel cubic structure.

Study the following findings and conclusions are can be summarized:

(i) The XRD patterns confirmed the Cu-Zn-RE ferrites are pluriphasic including cubic and orthorhombic. The substitutions of La for Fe in Cu-Zn ferrite mainly produce secondary $LaFeO_3$. The lattice parameter decreases with increasing La contents obeying Vagard's law. The bulk density is lower than the X-ray density, which is inevitable during ceramic processing and formed developing during the samples are preparation or the sintering process.

(ii) The substitution of Sm for in $(Cu_{0.5}Zn_{0.5}Fe_{2-x})Sm_xO_4$ ferrites revealed mainly the formation of secondary phase of composition $SmFeO_3$. The lattice parameter decreases with increasing Sm contents obeying Vagard's law. Bulk density of the ferrites increased with increasing Sm substitution, increased densification might be due to the appearance of excess Cu and Zn compared to Fe in the composition with respect Sm content.

(iii) The composition $(Cu_{0.5}Zn_{0.5}Fe_{1.95})La_{0.05}O_4$ showed best electromagnetic properties. A significant increase in initial permeability of the ferrite is found at small fraction of La (x = 0.05) substitution but increase of La content decrease initial permeability. The dispersion of the other compositions were at higher frequency range stable to x = 0.05 in the range 1kHz to 30MHz is constant initial permeability. Imaginary part of the complex permeability gradually decreased with frequency and attains state line at certain range of frequency.

(iv) The initial permeability decreases with increasing Sm substituted Cu-Zn ferrites monotonically. Decrease in permeability with Sm substitution might primarily be attributed to the increase in bulk density and may be due to secondary phase of $SmFeO_3$ segregated in the prepared samples. The imaginary permeability initially rises and suddenly decreases at low value at constant up to high frequency MHz range.

(v) Magnetization increases sharply at very low field (H < 1kOe) which corresponds to magnetic domain reorientation due to domain wall displacement and there after increase slowly up to saturation due to spin rotation for both rare earth La or Sm substituted Fe in Cu-Zn ferrites. The magnetization process is connected with soft magnetic behavior of magnetic material. Saturation magnetization decreases with increasing both La and Sm substituted Fe in Cu-Zn ferrites can be explained on the basis of cation distribution and exchange interaction A- and B-sites. Observed saturate value of Sm substituted ferrites is lower value that unsubstituted specimen seems that strong short range ferromagnetic ordering and frustration coexists with in the antiferromagnetic matrix.

(vi) Dielectric constant decreases with increasing frequency exhibiting normally dielectric behavior of ferrites like all the samples. All the figures shows the sample x = 0.1 showed the initially maximum dielectric constant and dispersion samples are shown in both La and Sm substituted Fe in with Cu-Zn ferrites. The increases in frequency enhance the hopping frequency of charge carriers, resulting in an increase in the conduction process, thereby decreasing the dielectric constant. Dielectric structure to be composed of the fairly well conducting ferrite grain.

5.2 Scope for Future Work

With the development and advancement of rare earth substituted ferrites a tremendous surge in research on miniaturization and high efficiency electronic devices is on rise. These modern devices exclusively need soft ferrite materials are used in inductors which form a basic requirement in high technology areas.

The scopes of the future works are proposed as:

(i) Different spinel ferrite systems to investigate the effect on lowering the sintering temperature are improving electromagnetic properties.

(ii) Fabrication and characterization of multilayer chip inductor using improved rare earth substituted Fe in Cu-Zn ferrites as stated.

(iii) AC and DC electrical properties may be studied.

(iv) SEM can be studied for better understand surface nature and domain wall motion.

Therefore future work on these types of systems may be carried out using electromagnetic properties such as permeability and resistivity is dependent on the densification and macrostructure of the ferrite.

REFERENCES

CHPATER-I

[1.1] Kulikowski J; "Soft magnetic ferrites development of stagnation", J. Magn. Magn. Mater., 41, 56 – 62, 1984.

[1.2] Snoek J. L.; "New developments in Ferromagnetism &Antiferromagnetism"; Annales de physique, 3, 137, 1948.

[1.3] Nakamura J.,Miyamoto T. and Yamada Y.; "Complex Permeability Spectra of Polycrystalline Li – Zn Ferrite and Application of EM – Eave Absorber"; J. Magn..Magn Mater., Vol.256, pp. 340 – 347, 2003

[1.4] Kin O. Low, Frank R. Sale, "electromagnetic properties Gel-derived Ni-Cu-Zn Ferrites" J. Magn. Magn. Mater., Vol.246, pp. 30 – 35, 2002.

[1.5] Khan Z. H., Sikder S. S., Hakim M. A., Saha D. K. and Noor S.; "Structural and Magnetic Properties of Cu-substitute Ni - Cu – Zn Ferrites", Journal of Engineering Science, 02, 81 – 85, 2011

[1.6] Rezlescu N., Rezlescu L., Popa P. D. and Rezlescu L.; "Influence of Additives on the Properties of a Ni – Zn ferrite with Low Curie point" J. Magn. Magn. Mater.; pp. 215 – 216, 2000

[1.7] Abdeen A. M.; "Electrical Conduction in Ni – Zn Ferrites", J. Magn. Magn. Mater., 185, 199, 1998

[1.8] Kin O. Low and Frank R. Sale; "Electromagnetic properties of gel-derived Ni-Cu-Zn ferrites", J. Magn. Magn. Mater. Vol.246, pp.30-45, 2002.

[1.9] Khan Z. H., MahbuburRahman M., Sikder S. S., Hakim M. A. and Saha D. K.; "Complex Permeability of Fe- deficient Ni – Zn – Zn Ferrites" Journal of Alloys and Compounds, 548, 208 – 215, 2013

[1.10] Seo S. H. and Oh J. H., "Effect of MoO_3 addition of sintering behaviors and magnetic properties of Ni-Cu-Zn ferrites for multilayer chip inductors." IEEE Transactions on magnetic, vol. 35, No. 5., 1999.

[1.11] Valenzuela R. ;Magnetic ceramics, Cambridge University Press, 1994.

[1.12] Murdock E. S., Simmons R. F., Davidson R.; Roadmap for 10 Gbit/in2 Media: Challenges. IEEE Trans. Magnetics, 28 (5)3078, 1992

[1.13] K. H. Maria, S. Choudhury, Journal of Bangladesh Academy of Sciences, **34** (2010) 1.

[1.14] Yang C. H., Kan D., Takeuchi I., Nagarajan V. and Seidel J; "Doping $BiFeO_3$: approaches and enhanced functionality", Phys. Chem. Chem. Phys., 14, 15953–15962, 2012.

[1.15] ManjurulHaque M. and Hakim M. A., "Thermal hysteresis of permeability of transport properties of Mn Substituted Mg-Cu-Zn ferrites." Journal of physics D. : Applied physics, vol. 41, 055007, pp 1-10, 2008.

[1.16] ManjurulHaque M., Huq M. and Hakim M. A., "Influence of CuO and sintering temperature on the microstructure properties of Mg-Cu-Zn Ferrites." J. Magn. Magn. Mater., Vol. 320, pp. 2792-2799, 2008.

[1.17] Ahmed M. A. Okasha N. and El-sayed M.M., "Enhancement of the physical properties of rare earth substituted Mn-Zn ferrites by Flash Method." Ceramic International, 33, 1, 49-58, 2007.

[1.18] Sun J., Li J and Sun G., "Effect of La_2O_3 and Gd_2O_3 on some properties of Ni-Zn Ferrite". J. Magn. Magn. Mater. 250, 20-24, 2002.

[1.19] Carter C. Barry, Norton M. Grant; Ceramic Materials: Science and Engineering, Springer. pp. 212–15, ISBN 0-387-46270-8, 2007

[1.20] Toshiyuki Suzuki, Termitsu Tanaka, Kaoru Ikemizu; "High density recording capability for advanced particulate media", J. Magn. Magn. Mater.,235, 159, 2001.

[1.21] GannakopoulouT., KompotiatisL.,KontogeogakosA., Kordas G.; "Microwave behavior of ferrites prepared via sol-gel method", J. Magn.Magn.Mater.,246, 360, 2002.

[1.22] Šoka Martin, Mariana Ušáková, ElemírUšák, RastislavDosoudil and JánLokaj;"Magnetic Properties Analysis of Rare-Earth Substituted Nickel Zinc Ferrites", IEEE Transactions On Magnetics, Vol. 50, No. 4, 2014.

[1.23] Khan Z. H., MahabuburRahman M. Sikder S. S., Hakim M. A., ShireenAkhter, Das H. N. and Anjuman B; "Thermal Hysteresis of Cu substitute $Ni_{0.28}Cu_{0.10+x}Zn_{0.62-x}Fe_{1.98}O_4$ ferrites", Advanced Chemistry letters, Vol.1, pp.1-6, 2013.

[1.24] Low K. O. and Sale F. R.; "Electromagnetic properties of Gel-derived Ni-Cu-Zn ferrites", J. Magn. Magn. Mater., 246, 30-35, 2002

[1.25] Hossain M. A., Khan M. N. I. and Sikder S. S.; "Structural Magnetic and Dielectric Behaviors of Y^{3+} Substituted Ni-Zn Ferrites", International Journal of Nano Science Trends and Technology, 1, 2, 1-19, 2017.

[1.26] Hossain M. A., Khan M. N. I. and Sikder S. S.; "Effect of Resistivity, Permeability and Curie Temperature of Rare Earth Metal Europium (Eu) Substitution on $Ni_{0.60}Zn_{0.40-x}Eu_xFe_2O_4$ (x = 0.05, 0.10, 0.15) Ferrites", ARPN Journal of Science and Technology, Vol.5, No.10, pp. 520-524, 2015.

[1.27] Costa A. C. F. M., Morelli M. R. and Kiminami R. H. G. A.; J. Mat. Sci. 39, 1773, 2004.

[1.28] Roy P. K. and Bena J., "Electromagnetic Properties of Samarium Substituted Ni-Cu-Zn Ferrite Prepared by Auto Combustion Method" J. Magn. Magn. Mater, 321(4), 247-251, 2009.

[1.29] Roy P. K., Nayak B. B. H. and Bera J., " Study on Electro –magnetic Properties of La Substituted Ni-Cu-Zn Ferrite Synthesized by Auto Combination Method." J. Magn. Magn. Mater, 320, 1128-1132, 2008.

[1.30] Sun J., Li J. and Sun G.; J. Magn. Magn. Mater., 25, 20, 2002.

[1.31] Rezlescu N., Rezlescu E., Popa P. D., Rezlescu L.; J. Alloys Compds., 657, 275, 1998.

[1.32] Jacoba S. E., Dukalde S., Bertorella H. R.; J. Magn. Magn. Mater., 253, 272, 2004.

CHAPTER-II

[2.1] Rare Earth Elements - Critical Resources for High Technology: United States Geological Survey; Fact Sheet 087-02.

[2.2] Rare Earths**;**United States Geological Survey, Mineral Commodity Summaries, 2014.

[2.3] Rezlescu N., Rezlescu E., Pasnicu C., Craus M. L.; J. Phys. Cond. Matter 6,5707, 1994.

[2.4] Satter A.A. and El- Shokrofy K. M.; J. Phys, IV ed. 245, 1997.

[2.5] Jing J., Liang-Chao L., Feng X.; Chin. J. Chem. 24, 1804, 2006.

[2.6] Jing J., Liang-Chao L., Feng X., J.; Rare Earths.25, 79, 2007.

[2.7] Vanuitert L. G., J. Chemi.Phys. 23, 1883, 1955.

[2.8] Kolekar C. B., Kamble P.N., Vaingankar A. S.; J. Bull. Mater. Sci. 18(2), 133,

[2.9] Jie S., Lixi W., Naicen X., Qitu Z., J. Rare Earths, 28, 445, 2010.

[2.10] Bahadur D., Giri J., Nayak B.B, Sriharsha T., Pradhan P., Prasad NK; 2J. Pramana Phys. 65, 663, 2005.

[2.11] Carter C. Barry; Norton, M. Grant, Ceramic Materials: Science and engineering, pp. 212-15. ISBN 0-387-46270-8, 2007.

[2.12] SmitJ., Wijn H. P.; J. Ferrites, John Wiley and Sons, New York, 1959.

[2.13] Rollin J. Parker; John Wiley and Sons, "Advances in Permanent Magnetism"; Inc., New York, 1990.

[2.14] Standly K. J.; "Oxide Magnetic Materials"; 2nd ed., Oxford University Press, 1972.

[2.15] Adams D.M.; "Inorganic Solids", John Willey, London, pp. 68, 1974.

[2.16] Standly K. J.; "Oxide Magnetic Materials", 2nd ed., Oxford University Press, 1972

[2.17] ChanR.W.,HassanP.,KrarerE.J.; "Materials Science and Technology," Vol.3B,VCH Publishers Inc.New York 1994.

[2.18] Chen C. W.; "Magnetism and Metallurgy of Soft Magnetic Materials"; New York 1977.

[2.19] Verway E. J. and Heilmann E. L.; Journal of Chem. Physics.15(4), 174, 1947.

[2.20] Van Uitert L. G.; J. Chem. Phys. 24(2), 1956.

[2.21] Merzbacher, Eugen; "Quantum Mechanics (3rd ed.)", pp. 372–3, 1998.

[2.22] Griffiths, David;"Introduction to Quantum Mechanics (2nd ed.)", pp. 183–4, 2005.

[2.23] Samokhvalov A.A.and Rustamov A. G.; SOV.Phys. Solid State, 6, 749, 1964.

Chapter III

[3.1] Kong L.B., Li Z. W., Lin G.Q. and Gan Y. B.; "Magneto-Dielectric properties of Mg-Cu-Co ferrites Ceramic: II Electrical, dialectical and magnetic properties", J. Am. Ceram. Soc., 90(7), 2014, 2007.

[3.2] Sharma S. K., Kumar R., Kumar S. Knobel M., Menses C.T., Kumar V. V. S., Reddy V. R. , Singh M. and Lee C. G.; " Role of inter partical interactions on the magnetic behavior of $Mg_{0.95}Mn_{0.05}Fe_2O_4$ ferrite nanoparticales"; J. Phys. Conden. Matter. , 20, 235214, 2008.

[3.3] Zahi S., Hashim M. and Daud A. R.; "Synthesis magnetic and microstructure of Ni-Zn ferrite by Sol-gen technique"; J. Magn. Magn.Mater., 308, 177, 2007.

[3.4] Hakim M. A., Saha D. K. and FazleKibria A. K. M. ; "Synthesis and temperature dependent structural study of nanocrystalline Mg- ferrite materials"; Bang. J. Phys., 3, 57, 2007.

[3.5] Bhaskar A., RajiniKanth B. and Murthy S. R.; "Electrical properties of Mn added Mg-Cu- Zn ferrites prepared by microwave sintering method"; J. Magn.Magn.Mater.; 283, 109, 2004.

[3.6] Yue Z., Zhou J.,Li L. and Gui Z.; " Effects of MnO_2 on the electro-magnetic properties of Ni-Cu-Zn ferrites prepared by sol-gel auto combustion"; J. Magn. Magn.Mater., 233, 224, 2001.

[3.7] ChenC. W.; "Magnetism and Metallurgy", Soft Mag. Mat., North-Holland Pub. Com. XV, 288,1977.

[3.8] KittelC.; "Introduction to Solid State Physics"; 7^{th} edition, John Wiley and sons, Inc., Singapore ,1996.

[3.9] Gadkari A. B., Shinde T. T. and Vasambekar P. N. ; "Structural and Magnetic properties of nanocrystalline Mg-Cd ferrites prepared by oxalate Co-precipitation methods"; J. Mater. Sci. Mater. Electron, 21(1), 96 - 103, 2010.

[3.10] Tahir Abbas, IslamM. U. and AshrafM. ;Ch; Mod. Phy.Letts.B 9(22), 1419.1995.

[3.11] Balayachi A., Dormann J. L. and Nogues M.; "Critical analysis of magnetically semi disordered systems: critical exponents at various transitions", J. Phys. Condens. Matter.10, 1599, 1998.

[3.12] Slick P. I.; " Ferrites for Non-microwave applications", ferromagnetic materials, Ed. E. P. Wolfarth, North Holland Pub Co_2, 1980

[3.13] B. Creek, Advantage Sintered Metals, Michigan, USA.

[3.14] Cullity B. D.; "Introduction to Magnetic Materials'; Addison –Wesley publishing company, Inc. 1972

[3.15] NelsonJ. B., RileyD. P.; "An experimental investigation of extrapolation methods in the derivation of accurate unit-cell dimensions of crystals", Proc. Phys. SOC London 57, 160, 1945.

[3.16] Smit J. and WijinH. P.; Ferrites, Wiely New York, 250, 1959.

[3.17] Simon Forner; "Versatile and sensitive Vibrating Sample Magnetometer", Rev. Sci. Instr. 30, P.548, 1959

Chapter IV

[4.1] Costa A. C. M., Morelli M. R. and Kiminami R. H. G. A.; "Microstructure and Magnetic properties of Ni-Zn-Sm ferrites", Ceramica, 49:168, 2003.

[4.2] Mohamed O., Hemeda M. M., Barbkat M. M. and Hemeda D. M.; "Structural, electrical and spectral studies on rare earth orthoferrites $La_{1-x}Nd_xFe_2O_3$", Turk. J. Phy., 27:537, 2003.

[4.3] Calderon-Qritiz E., Perales-Perez O., Voyles P., Guterrez G. and Tomar M. S.; "$Mn_xZn_{1-x}Fe_{2-y}R_yO_4$ (R = Gd, Eu) ferrites nanocrystals for potential magnetocaloric application", [in] ENS'07, Paris 2007.

[4.4] Ashok Gadari, TukaramShinde and PramodVasambekar; "Influence of rare-earth ions on structural and magnetic properties of $CdFe_2O_4$ ferrites", RARE METALS, Vol. 29, No.2, April 2010.

[4.5] Sun J., Li J. and Sun G.; "Effects of La_2O_3 and Gd_2O_3 on some properties of Ni-Zn ferrite", J. Magn.Magn.Mater., 250, 20, 2002.

[4.6] Nelson J. B., Riley D. P.; "An experimental investigation of extrapolation methods in the derivation of accurate unit-cell dimensions of crystals"; Proc. Phys. Soc. London 57, 160, 1945.

[4.7] Vegard L.; "Die constitution der mischkristalle und die raumfulling der atome", Z. Phys. 5, 17, 1945.

[4.8] Smit J., Wijn H. P. J.; "Ferrites", Wiley New York, p.143.4.4, 1959.

[4.9] John Berchamans L., KalaliSelvan R., Selva Kumar P. N.andAugustin C. O.; "structural and electrical properties of $Ni_{1-x}Mg_xFe_2O_4$synrhesized by citrate gel process',J. Magn. Magn.Mater.279, 10, 2004.

[4.10] Yang Z.-H., Gong Z.-Q., Li H.-X., Ma Y.-T.andYang Y.–F.; "Synthesis of Ni_zn Ferrites and its Microstructure and Magnetic Properties", Journal of Central South University of Technology, Vol.13, No.6, pp.618-623, doi:10.1007/s11771-006-0004-x., 2006.

[4.11] Gorter E. W.; Philips Res. Rep. 9, 295, 1954.

[4.12] Verma A., Chatterjee R.; "Effect of zinc concentration on the structural, electrical and magnetic properties of mixed Mn-Zn and Ni-Zn ferrites synthesized by the citrate precursor technique"; J. Magn. Magn.Mater.306, 313 – 320, 2006.

[4.13] Shrotri J. J., Kulkarni S. D., Deshpande C. E., Date S. K.; "Effect of Cu substitution on the magnetic and electrical properties of Ni-Zn ferrite synthesized by soft chemical method", Mater. Chem. Phys., 59, 1, 1999.

[4.14] Overshott K.; "The causes of the anomalous cross in amorphous ribbon materials"; IEEE Trans. Magn.17, 2698, 1981.

[4.15] Brockman F. G., Dowling P. H.andSteneck W. G.; "Dimensional effects resulting from a high dielectric constant found in a ferromagnetic ferrite", Phys. Rev. 77, 85, 1950.

[4.16] Kolekar C. B., Kamble P. N., Kulkarni S. G.andVaingankar A. S.; "Effect of Gd^{3+} substitution on dielectric behavior and copper-cadmium ferrites"; J. Matter. Sci. 30, 5784, 1995.

[4.17] ZhenxingYue, Zhou Ji, ZhilunGui and Longtu Li; "Magnetic and electrical properties of low temperature sintered Mn-doped Ni-Cu-Zn ferrites", J. Magn. Magn.Mater.264, 258, 2003.

[4.18] Bellad S. S. and Chougula B. K.; "Composition and frequency dependent dielectric properties of Li-Mg-Ti ferrites", Mater. S. Chem. Phys., 66, 58, 2000.

[4.19] Bhaskar A., RajiniKanth B., Murthy S. R.; "Electrical properties of Mn added Mg-Cu-Zn ferrites prepared by microwave sintering method"; J. Magn. Magn.Mater., 283, 109, 2004.

[4.20] ZhenxingYue, Zhou Ji, Longtu Li, Xiaolui Wang and ZhilunGui; "Effect of copper on the electromagnetic properties of Mg-Zn-Cu ferrites prepared by Sol-gel auto-combustion method", Mater. Sci. Eng., B 86, 64, 2001.

[4.21] Nutan Gupta, Kashyap S. C.Dube and D. C.; "Dielectric and Magnetic properties of Citrate route processed Li-Co Spinel ferrites", Phys. Stat. Solidi(a), 204(7), 2007.

[4.22] Maxwell J.; 1873, "Electricity and Magnetism"; Vol.1 Oxford University Press.London Wanger K 1913 Ann. Phys. 40 817.

[4.23] Venugopal Reddy P., SeshagiriRao T.; "Dielectric behavior of mixed Li-Ni ferrites at low frequencies", J. Less. Common Met., 86, 255, 1982.

CONFERENCE PRESENTATION

P. K. Mondal,M. A. Hossain, M. N. I. Khan and S. S. Sikder,; "Study of the Structural and Magnetic Properties of Lantanum (La) and Samarium (Sm) Incorporated Cu-Zn Ferrites", International Conference on Physics – 2018, 08 -10 March, 2018, University of Dhaka, Dhaka-1000, Bangladesh

P. K. Mondal, M. A. Hossain, M. N. I. Khan and S. S. Sikder,; "Investigate the Influence of Sm in the Electrical Transport and Magnetic Properties of $(Cu_{0.5}Zn_{0.5}Fe_{2-x})Sm_xO_4$ Ferrites", Conference on Weather Forecasting & Advances in Physics-2018,11-12 May,2018,KUET,Bangladesh.

P. K. Mondal, M. A. Hossain, M. N. I. Khan and S. S. Sikder,; "Studies on Structural and Complex Permeability of $(Cu_{0.5}Zn_{0.5}Fe_{2-x})La_xO_4$ Ferrites Synthesized by Double Sintering Technique", Conference on Weather Forecasting & Advances in Physics-2018,11-12 May,2018,KUET,Bangladesh.